

AD-A270 823



# The Deposition of Electro-Optic Films on Semiconductors

(2)

ONR Contract No. N0014-91-J-1307

**DTIC**  
**S** **ELECTE** **D**  
OCT 18 1993  
**A**

**Periodic Project Report**  
Covering the period January 1, 1992 - April 30, 1993

**Principal Investigators:**  
Angus I. Kingon      Orlando H. Auciello      Klaus J. Bachmann

North Carolina State University  
Department of Materials Science and Engineering  
Raleigh, NC. 27695-7907  
(919) 515-2867

This contract report was prepared by A. I. Kingon., Rene R. Woolcott,  
Alice F. Chow, and Thomas M. Graettinger.

This document has been approved  
for public release and sale; its  
distribution is unlimited.

The views and conclusions contained in this document are those of the  
authors and should not be interpreted as necessarily representing the  
official policies, either expressed or implied, of the Office of Naval Research  
or the U.S. Government.

**93-24221**



93 10 14 034

REPORT DOCUMENTATION PAGE			Form Approved OMB No. 0704-0188	
Public reporting burden for this collection of information is estimated to average 1 hour per response, including the time for reviewing instructions, searching existing data sources, gathering and maintaining the data needed, and completing and reviewing the collection of information. Send comments regarding this burden estimate or any other aspect of this collection of information, including suggestions for reducing this burden to Washington Headquarters Services, Directorate for Information Operations and Reports, 1215 Jefferson Davis Highway, Suite 1204, Arlington, VA 22202-4302, and to the Office of Management and Budget Paperwork Reduction Project (0704-0188), Washington, DC 20503.				
1. AGENCY USE ONLY (Leave blank)		2. REPORT DATE October 8, 1993		3. REPORT TYPE AND DATES COVERED Interim: January 1, 1992-April 30, 1993
4. TITLE AND SUBTITLE The Deposition of Electro-Optic Films on Semiconductors			5. FUNDING NUMBERS N0014-91-J-1307 1131 N00179 N66005 4B855	
6. AUTHOR(S) Angus I. Kingon				
7. PERFORMING ORGANIZATION NAME(S) AND ADDRESS(ES) North Carolina State University Hillsborough Street Raleigh, NC 27695			8. PERFORMING ORGANIZATION REPORT NUMBER N0014-91-J-1307	
9. SPONSORING/MONITORING AGENCY NAME(S) AND ADDRESS(ES) Office of Naval Research Code 1512: JMG Ballston Tower One 800 North Quincy Street Arlington, VA 22217-5660			10. SPONSORING/MONITORING AGENCY REPORT NUMBER	
11. SUPPLEMENTARY NOTES				
12a. DISTRIBUTION/AVAILABILITY STATEMENT  Approved for Public Release; Distribution Unlimited			12b. DISTRIBUTION CODE	
13. ABSTRACT (Maximum 200 words)  High quality potassium niobate thin films have been grown on magnesium oxide, spinel, potassium tantalate, and sapphire by Ion Beam Sputter Deposition. The effects of substrate preparation, process conditions, and film stoichiometry are being correlated with optical properties. The factors contributing to optical losses is the present focus of our research since low losses are an essential criteria for building device structures. Electro-optic properties of KNbO <sub>3</sub> films on MgO are found to be similar to bulk, although the scattering losses are very high for these films. In comparison KNbO <sub>3</sub> films grown on KTaO <sub>3</sub> exhibit low losses of less than 8 dB, while losses for films on spinel showed to be in between those two. The variety of substrates provide us with differences in lattice mismatch, refractive index mismatch, surface morphologies, and microstructure, all of which influence loss characteristics.				
14. SUBJECT TERMS potassium niobate, magnesium oxide, spinel, potassium tantalate, sapphire, Ion Beam Sputter Deposition, optical losses, electro-optic thin films.			15. NUMBER OF PAGES 40	
			16. PRICE CODE	
17. SECURITY CLASSIFICATION OF REPORT UNCLAS		18. SECURITY CLASSIFICATION OF THIS PAGE UNCLAS		19. SECURITY CLASSIFICATION OF ABSTRACT UNCLAS
				20. LIMITATION OF ABSTRACT SAR

# Interim Report Distribution List

"The Deposition of Electro-Optic Films on Semiconductors"

ONR Contract No. N0014-91-J-1307

January 1, 1992 - April 30, 1993

Addressee Unclassified Unliimited

Wallace A. Smith 3  
Scientific Officer Code: 1131  
Office of Naval Research  
800 North Quincy Street  
Arlington, Virginia 22217-5000

Administrative Grants Officer 1  
Office of Naval Research  
Resident Representative N66005  
Administrative Contracting Officer  
The Ohio State Univ. Research Ctr  
1314 Kinnear Road  
Columbus, OH 43212-1194

Director, Naval Research Laboratory 1  
Attn: Code 2627  
Washington, DC 20375

Defense Technical Information Center 2  
Building 5, Cameron Station  
Alexandria, Virginia 22304-6145

Angus I Kingon, Principal Investigator 1  
Orlando Auciello, Principal Investigator 1  
Klaus K Bachmann, Principal Investigator 1  
North Carolina State University  
Box 7919  
Raleigh, NC 27695-7919

Accession For	
NTIS	CRA&I <input checked="" type="checkbox"/>
DTIC	TAB <input type="checkbox"/>
Unannounced	<input type="checkbox"/>
Justification	
By	
Distribution /	
Availability Codes	
Dist	Avail and/or Special
A-1	

RECEIVED 12/12/93

# 1. Introduction

This report covers research undertaken under sponsorship of the Office of Naval Research. The report covers the period from 1 January, 1992 until 30 April, 1993. The reporting period is longer than the usual 12 months in order to bring it in line with the project period (1 Jan 1991 - 30 April 1994). The final year report will therefore cover the 12 month period 1 May, 1993 to 30 April, 1994.

The total project objectives include the deposition of  $\text{KNbO}_3$  thin films on silicon, sapphire and gallium arsenide substrates; the design of simple electro-optic devices; and the addressing of issues of scaleup.

We need to highlight two important aspects of the work of this period.

1) The optical aspects of the research have focused upon measuring and minimizing the optical losses in the  $\text{KNbO}_3$  films in guided wave modes. We have come to the realization that there is a lack of understanding of the parameters which control the losses. As a result, we have recently focused our efforts to address this issue. We have therefore expanded the study to include the deposition and characterization of  $\text{KNbO}_3$  on a wider range of substrates. These substrates have been selected both for their relevance for devices and for the understanding that they could provide regarding optical losses. Thus they provide differences in lattice mismatch, refractive index mismatch, surface morphologies, and  $\text{KNbO}_3$  microstructures. Results to date are briefly discussed in the following sections.

2) An addendum to the program was initiated 1 October, 1992. This involves a collaboration between NCSU and DuPont. The rationale is the focusing of the project upon possible devices by making use of DuPont's current activities in, and links with, the commercial sector. The collaboration is being undertaken via a post-doctoral research associate, Dr. Thomas Graettinger. This collaboration has proved fruitful. Further details are presented in the following sections.

The accomplishments of the period are summarized below. Further details can be found in the publications which are included as Appendices.

## **2. Accomplishments - NCSU**

### **2.1 Background**

Thin films of  $\text{KNbO}_3$  were grown on  $\text{MgO}$ ,  $\text{MgAl}_2\text{O}_4$  (spinel),  $\text{KTaO}_3$ , and  $\text{Al}_2\text{O}_3$  (sapphire) single crystal substrates and buffer layers of  $\text{MgO}$  were deposited on Si, GaAs, and  $\text{Al}_2\text{O}_3$ . As a result of the optical characterization of the electro-optic films it has been shown that optical losses of films grown on differing substrates vary considerably for waveguide applications. The use of  $\text{KNbO}_3$ 's high nonlinear susceptibility for second harmonic generation (SHG) shows great promise for frequency doubling. The key is the optical waveguide's loss characteristic and it has been found from films grown on single crystals that lattice mismatch, interface roughness, refractive index match, twin formation, and the nature of low angle grain boundary tilt and twist can all severely affect such losses. However, the relative (or direct) contributions of each of these features on the loss must still be established before device structures on semiconductors can be optimized. This is a focus of ongoing research.

### **2.2 Processing of $\text{KNbO}_3$ Thin Films**

High quality potassium niobate thin films have been grown by a unique ion beam sputter deposition process. Rotating targets of potassium superoxide and niobium metal alternately exposed to an ion beam produce interdiffusing layers to form  $\text{KNbO}_3$  films. A quartz crystal resonator provides thickness feedback and thus, interdiffusion layer thickness and film composition can be accurately controlled. Growth temperatures vary between  $600^\circ\text{C}$  to  $750^\circ\text{C}$  to produce epitaxial and visually transparent films.

The effects of predeposition annealing of the substrates, interdiffusion layer thickness, processing temperature, and film stoichiometry are being correlated with optical properties.

## 2.3 Characterization of KNbO<sub>3</sub> Thin Films

X-ray diffractometry was performed routinely on samples to identify film orientation and any second phases. Transmission electron microscopy on planar view and cross section samples reveals interface roughness and microstructure information such as, twin domains, second phase regions, and grain size. Atomic force microscopy (AFM) provides surface roughness information before and after deposition. Rutherford backscattering spectroscopy (RBS) reveals thickness and composition data as well as epitaxial integrity through channeling techniques. High resolution topological grain and defect features are exhibited by Field emission scanning electron microscopy (FESEM).

Layer by layer growth of reactive ion beam sputter deposited KNbO<sub>3</sub> thin films was optimized to achieve near bulk values of the refractive index and birefringence shift. The [110] orthorhombic KNbO<sub>3</sub> films on [100] cubic MgO have an average refractive index of 2.2808 in TE mode and 2.2034 in TM mode. These compare to calculated bulk values for TE and TM modes of 2.2756 and 2.2221 respectively. All of these optical properties are excellent. The average birefringence shift  $[-\Delta(\Delta n)]$  at an applied field of 200 V/mm is  $3 \times 10^{-3}$ . The transverse effective electro-optic tensor's net coefficient value is approximately equal to  $350 \times 10^{-12}$  m/V ( $\pm 35 \times 10^{-12}$  m/V). This compares to a computed bulk value of  $325 \times 10^{-12}$  m/V ( $\pm 26 \times 10^{-12}$  m/V). All of these optical properties are excellent. However, scattering losses are very high for these films and pole figure plots indicate a significant  $1\frac{1}{2}^\circ$  grain tilt. X-ray diffraction patterns also reveal the presence of (221) tetrahedral twin domains. It should be noted here that the lattice mismatch to MgO is about 5.8%. In the case of films grown on KTaO<sub>3</sub> where the lattice mismatch is about 0.5%, the scattering losses are  $\leq 8$  dB. Thus far, films grown on spinel seem to lie between these two but the relatively low refractive index of MgAl<sub>2</sub>O<sub>4</sub> and MgO ( $n = 1.73$ ) will tend to enhance radiant loss as this scales with difference of the squares of the film and substrate indices. This is pointed out and discussed in the reference included as Appendix 3.

## **2.4 Buffer Layers on Silicon, Gallium Arsenide, and Sapphire**

Preferentially oriented [100] magnesium oxide buffer layers have been grown on sapphire (1102), silicon (100), and gallium arsenide (100) as documented by XRD and TEM electron diffraction patterns. Careful substrate preparation and unique deposition conditions particular to our ion beam system are necessary, particularly for the latter two substrates due to surface oxides. Native oxide of silicon deters epitaxial thin film growth and thus, a hydrogen terminated surface is chemically created on the silicon prior to entering a high vacuum setting. Nevertheless, silicon oxidizes upon heating to the MgO deposition temperature of 450-550°C and therefore highly oriented films are difficult to grow. On GaAs, the substrate is ramped up to 620°C for 2 min. prior to deposition to remove its oxide layer and there after cooled to the MgO deposition temperature for growth. Meanwhile, MgO growth on sapphire gave much more highly oriented films and without a complex surface preparation procedure. We selected the substrate orientation to be (1102) r-cut with a four degree off axis tilt which we calculated from atomic modeling to provide a good lattice match with (100) MgO. In light of the high quality MgO buffer layer on sapphire, silicon-on-sapphire applications will be explored.

## **3. Accomplishments - DuPont/NCSU Collaboration**

### **3.1 Background**

The goals of the NCSU/DuPont collaboration include the following:

- 1) Transfer ion beam expertise from NCSU to DuPont.
- 2) Determine the microstructural-optical properties relationships.
- 3) Expand the scope of the current NCSU work to other materials.

For the period 1 October, 1992 through 30 April, 1993 the research plan called for:

- 1) Deposition of  $\text{KNbO}_3$  thin films at DuPont using the ion beam sputter co-deposition system.
- 2) Deposition of  $\text{LiTaO}_3$  using the DuPont deposition system.
- 3) Investigation of chemical composition and microstructure of co-deposited films using Rutherford Backscattering Spectrometry, X-ray diffractometry, and Transmission electron microscopy.
- 4) Measurement of optical losses in  $\text{KNbO}_3$  films from NCSU.

The accomplishments of the collaboration may be as summarized in the following sections.

### **3.2 Final development and initial testing of ion beam sputter co-deposition system.**

During the period 1 October, 1992 through 31 December, 1992 final development/ installation and initial testing of the ion beam sputter co-deposition system at DuPont was completed. The system consists of a high vacuum stainless steel chamber containing three independent ion source-target pairs for co-sputtering material onto a single 3 inch substrate. The substrate is heated by quartz lamps to a maximum temperature of  $900^\circ\text{C}$ . In addition to the 3 primary sputtering ion sources, a fourth ion source was installed for ion assisted growth. This source provides direct low-energy ion bombardment of the growing film which has been shown by others to be a very useful tool for modifying microstructures and physical properties, and for lowering the deposition temperature for high quality thin film growth. The deposition system also includes three quartz crystal resonators, one of which monitors the sputtered flux from each of the three sputtering targets. A personal computer monitors the feedback from the resonators and has the ability to change the ion beam current on each target to maintain a desired sputtered flux rate and thus achieve correct chemical stoichiometry.

### **3.3 Deposition of $\text{KNbO}_3$ thin films.**

Drawing upon the expertise developed at NCSU,  $\text{KNbO}_3$  thin films were grown at DuPont using the co-deposition system. Epitaxial (110) oriented single phase  $\text{KNbO}_3$  thin films were grown on  $\text{MgO}$  (001) single crystal

substrates. A six inch diameter elemental niobium target and a six inch diameter potassium superoxide ( $\text{KO}_2$ ) target were co-sputtered to achieve stoichiometric epitaxial  $\text{KNbO}_3$  films. Films were deposited between  $600^\circ\text{C}$  and  $650^\circ\text{C}$  with a background pressure of  $1-2 \times 10^{-4}$  torr molecular oxygen. Primary sputtering ion energies were kept in the range of 500-1000 eV to minimize damage to the growing film from high-energy backscattered ions. Rutherford backscattering spectrometry (RBS) was used to determine the cation stoichiometry and thickness of the films. This RBS analysis was performed at the University of Pennsylvania in Philadelphia. Films deposited at NCSU were also analyzed at U. Penn. providing an independent measurement to the analysis done at the University of North Carolina at Chapel Hill. Results of the independent analyses agreed very well.

### **3.4 Film epitaxy studies using x-ray diffraction.**

To use a thin film as a medium for second harmonic generation, phase matching of the fundamental and second harmonic waves must occur. Normally this is only accomplished in certain crystallographic directions of a crystal. Therefore, it is desirable to produce a thin film that is a single crystal, requiring in-plane orientation of the film. The standard x-ray diffractometer theta-two theta scan is a powerful technique for identification of phases and for determining if any preferential orientation exists in a film. However, the standard diffraction pattern reveals nothing about the in-plane orientation of the film. In order to investigate the in-plane orientation of the  $\text{KNbO}_3$  thin films from both NCSU and DuPont, a pole figure rotation stage in combination with an x-ray diffractometer was used. This apparatus has the ability to probe crystal planes which are not parallel to the substrate surface. Analysis of the films using this apparatus revealed that the  $[110]$  axes of the films are tilted along the cubic directions of the  $\text{MgO}$  substrate by as much as 1.5 degrees. Films deposited at both NCSU and DuPont exhibit this behavior suggesting that the tilt is a substrate influenced characteristic and not related to the deposition method. The tilt is thought to be a strain accommodation mechanism produced as a result of the relatively large lattice mismatch between  $\text{KNbO}_3$  and  $\text{MgO}$  (6%). In addition, the tilt is

an indication that in-plane rotation exists in the films. This in-plane rotation must be overcome for efficient phase matching to be possible in these films.

### **3.5 Optical characterization of the $\text{KNbO}_3$ thin films.**

The indices of refraction of NCSU and DuPont  $\text{KNbO}_3$  thin films were measured using the prism coupling m-line technique at DuPont. NCSU and DuPont films supported both TE and TM guided modes. The measured indices ( $n_{\text{TE}} = 2.286$ ,  $n_{\text{TM}} = 2.202$  NCSU;  $n_{\text{TE}} = 2.221$ ,  $n_{\text{TM}} = 2.198$  DuPont) compare very closely to the bulk values of  $\text{KNbO}_3$  for equivalent orientation. Birefringence was not observed in the plane of the films which substantiates the earlier conclusion that in-plane rotation exists in the films.

A fiber probe was prepared at DuPont to measure the optical propagation losses in the  $\text{KNbO}_3/\text{MgO}$  films. However, scattering was too large in the films and prevented use of the probe.

### **3.6 Deposition of KTP films.**

DuPont has identified potassium titanyl phosphate ( $\text{KTiOPO}_4$ , KTP) as an important material for non-linear optical applications. Initial work has been done toward depositing thin films of this material using the co-sputtering deposition system. A stoichiometric KTP pressed powder target was used for the initial experiments. Depositions in a molecular oxygen background resulted in potassium and phosphorus deficient films on room temperature and heated y-cut quartz substrates. Potassium superoxide, titanium, and titanium phosphide (TiP) targets have since been obtained and will be used in the future for co-deposition experiments.

## **Publications**

- Appendix 1      "Optical Characterization of Potassium Niobate Thin Film Planar Waveguides," Thomas M. Graettinger and Angus I. Kingon, MRS Symposium Proceedings, Ferroelectric Thin Films II, Vol 243, (MRS Fall 1991), p. 557.
- Appendix 2.      "Ion-Beam Reactive Sputter Deposition of MgO Thin Films on Silicon and Sapphire Substrates," Alice F. Chow, Shang Hsieh Rou, Daniel J. Lichtenwalner, Orlando Auciello, and Angus I. Kingon, MRS Symposium Proceedings, Materials Modification by Energetic Atoms and Ions, Vol 268, (MRS Spring 1992, Pittsburgh, PA), p. 253-258.
- Appendix 3.      "Growth, Microstructures and Optical Properties of  $\text{KNbO}_3$  Thin Films," T.M. Graettinger, P.A. Morris, Rene R. Woolcott, F.C. Zumsteg, A.F. Chow, and A.I. Kingon, MRS Symposium Proceedings, Ferroelectric Thin Films III, Vol 310 (MRS Spring 1993, Pittsburgh, PA), (in press), (invited talk).
- Appendix 4.      "Ferroelectric Materials For Nonlinear Optical Devices," P.A. Morris, The Eighth International Meeting on Ferroelectricity, (August 1993), (invited talk).

## **Appendix 1**

## OPTICAL CHARACTERIZATION OF POTASSIUM NIOBATE THIN FILM PLANAR WAVEGUIDES

THOMAS M. GRAETTINGER AND A. I. KINGON

North Carolina State University  
Dept. of Materials Science and Engineering  
Raleigh, NC 27695-7919

### ABSTRACT

Initial results of the waveguiding properties of  $\text{KNbO}_3$  thin films are presented. The refractive indices of epitaxial films deposited on single crystal magnesium oxide substrates have been measured. Additionally, these films have been used as the basis for modelling a potassium niobate thin film phase modulator. Results of the model are compared with existing technology.

### INTRODUCTION

Ferroelectric materials possess great potential for use in integrated optics due to their strong electro-optic and non-linear optical effects. Thin film fabrication methods for these materials are currently the subject of much study. High quality, transparent, low loss films must be grown for application into device structures. An important parameter in determining the quality of ferroelectric thin films is the refractive index which can be measured using several techniques including the prism coupling method. Lower than bulk values of refractive index often indicate porous, off-stoichiometry, or poor quality thin films unsuitable for devices.

Of the materials being considered for use in integrated optic switching devices, potassium niobate ranks very highly due to its very strong electro-optic effect and moderate dielectric susceptibilities. This ferroelectric has been difficult to grow in bulk crystalline form, but thin films have recently been deposited making it attractive for the integrated optic applications.

### EXPERIMENTAL PROCEDURE

Potassium niobate thin films were prepared by an ion beam sputtering technique described previously.[1] Sequential deposition of very thin layers of potassium oxide and niobium oxide from potassium superoxide pressed powder and niobium metal targets resulted in the formation of the desired perovskite phase. Film composition and thickness were determined from Rutherford Backscattering (RBS) spectra. The single phase nature of the films was determined from X-ray Diffractometer (XRD) scans of the films and Selected Area Diffraction (SAD) patterns from transmission electron microscope (TEM) specimens.

Optical guided waves were launched into the thin films using a symmetrical rutile prism coupler [2] with a base angle of  $60^\circ$  and refractive index of 2.8659. The prism and film were clamped together to achieve a good coupling spot and the clamped assembly was mounted on a goniometer. A helium-neon laser ( $\lambda = 632.8 \text{ nm}$ ) was focused on the coupling spot at the prism-film interface. The light was polarized in order to launch only TE modes in the films. A schematic of the system is shown in figure 1. The reflected beam from the prism coupler was detected with a silicon photodiode and its signal monitored with a chart recorder. The prism coupling assembly was rotated until a sharp decrease in the reflected beam intensity was detected signaling the launching of a guided mode. The coupling angle relative to normal incidence of the input beam on the entrance face of the prism was measured. A computer was used to perform the iterative calculation necessary to determine the refractive index of the film from the coupling angle and the film thickness.[3]

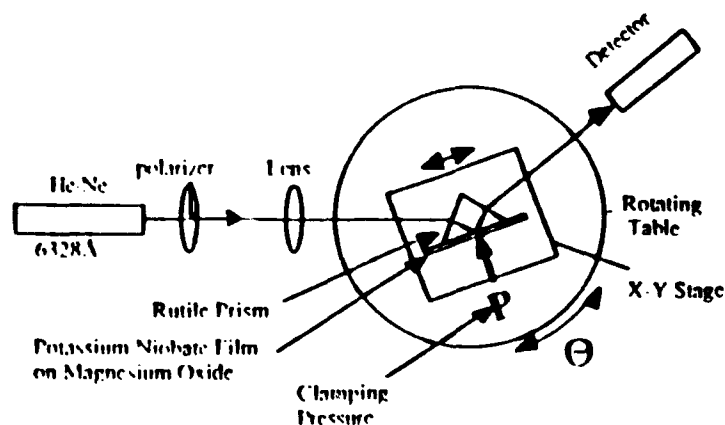


Figure 1. Prism coupling system used to determine thin film refractive index.

## RESULTS AND DISCUSSION

### Guided-wave characterization

Epitaxial b axis oriented orthorhombic potassium niobate thin films were grown on single crystal magnesium oxide (001) substrates. Magnesium oxide was chosen for these experiments because of its close lattice match with  $\text{KNbO}_3$  and its refractive index of 1.73. A low refractive index relative to the thin film is necessary to prevent guided-wave losses into the substrate. In addition, the crystallographic orientation of the films on MgO is suitable to make use of one of the larger coefficients of the electro-optic tensor in integrated optic devices.

The compositions of the films were analyzed using RBS spectra. Figure 2 shows a representative spectra of the  $\text{KNbO}_3$  films. All films measured were slightly potassium deficient with a potassium to niobium ratio in the range of  $0.85:1 < \text{K:Nb} < 0.95:1$ . As stoichiometric potassium niobate ( $\text{K:Nb} = 1:1$ ) is reached and exceeded the films roughen and change from transparent to translucent. The single phase nature and the orientation of the films can be seen from the X ray diffraction scan shown in figure 3. The epitaxial relationship between the films and the substrate was verified from SAD patterns of TEM samples.

The refractive index of the  $\text{KNbO}_3$  thin films was determined by measuring the angle at which guided modes were launched into the films using a prism coupler. Only the  $\text{TE}_0$  mode was launched because the film thickness was in the range 2000 to 2500 angstroms, determined from the RBS spectra. The coupling angle was determined by detecting a sharp decrease in the intensity of the beam reflected from the prism-film interface as the incident angle was changed as shown in figure 4. At 632.8 nm the refractive index of the films was determined to be 2.28. This result is in good agreement with published values of the refractive index of bulk orthorhombic  $\text{KNbO}_3$  and indicates that the films are dense and of high quality. For b-axis (010) oriented films, the refractive index for TE polarized optical waves should lie in the range between the refractive indices in the a-, (100), and c-, (001), crystallographic directions, 2.28 to 2.17, respectively.

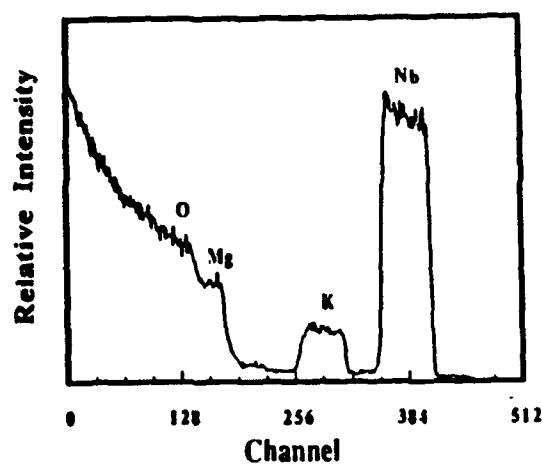


Fig. 2. Rutherford Backscattering spectra of a  $\text{KNbO}_3$  thin film.

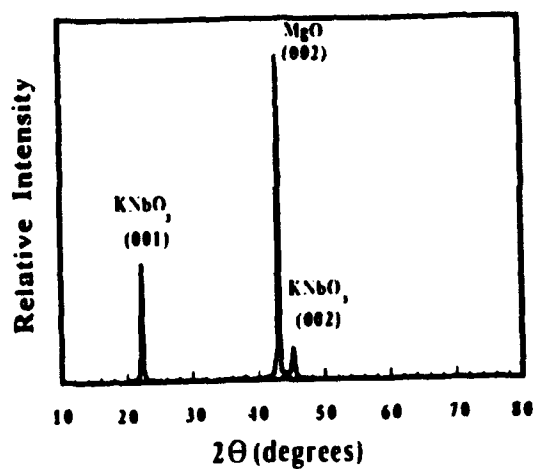


Fig. 3. X-ray diffraction scan of a  $\text{KNbO}_3$  thin film.

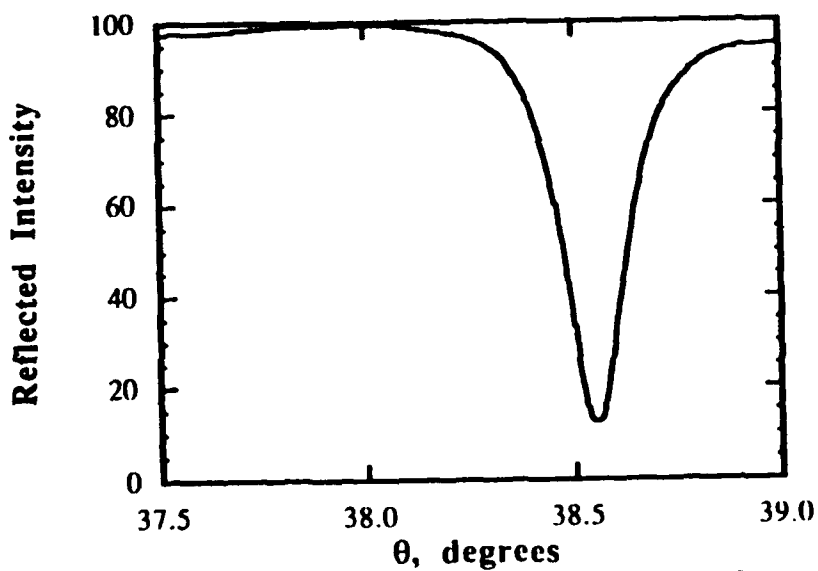


Fig. 4. The intensity of reflected light from a prism coupler as a function of the index of refraction of a propagating mode which is proportional to the angle of incidence.

### KNbO<sub>3</sub> Phase Modulator Model

To demonstrate the utility of the ion beam sputter-deposited potassium niobate thin films, a waveguide electro-optic modulator based on the thin films was modeled. High quality films of KNbO<sub>3</sub> have been deposited on single crystal magnesium oxide ((001)). These films have been grown heteroepitaxially on the MgO surface with P<sub>5</sub> of the orthorhombic KNbO<sub>3</sub> oriented in the plane of the film. These films will serve as the basis for the electro-optic phase modulator model. There are four equivalent directions for P<sub>5</sub> in the plane of the film, but, for the purposes of this model, a film whose polarization vectors all point in a single direction will be considered. The results of the model will then be compared to existing technology.

The optical indicatrix for KNbO<sub>3</sub>, a biaxial material, can be written as[4]

$$B_1 x_1^2 + B_2 x_2^2 + B_3 x_3^2 + 2B_4 x_2 x_3 + 2B_5 x_1 x_3 + 2B_6 x_1 x_2 = 1 \quad (1)$$

where  $B_i = 1/n_i^2$ , and the subscripts use contracted indices. Deformation of the optical indicatrix occurs as a result of the electro-optic effect when an electric field is applied to the crystal. Potassium niobate belongs to the crystal class mm2, so the deformation of the indicatrix obeys the relation

$$(B_1 + r_{11}E_1)x_1^2 + (B_2 + r_{22}E_1)x_2^2 + (B_3 + r_{33}E_1)x_3^2 + 2r_{12}E_1x_2x_3 + 2r_{31}E_1x_1x_3 = 1 \quad (2)$$

For the use of the KNbO<sub>3</sub> films discussed above in guided-wave devices, light must propagate in the 1-3 plane. The guided wave may be polarized either TE (in the 1-3 plane) or TM (normal to the 1-3 plane) in a single mode waveguide. Thus, for these thin films the fourth term in Eq. (2) is of no consequence since light can not be polarized in the 4 direction.

For a field applied along x<sub>3</sub>, Eq. (2) reduces to

$$(B_1 + r_{11}E_3)x_1^2 + (B_2 + r_{22}E_3)x_2^2 + (B_3 + r_{33}E_3)x_3^2 = 1 \quad (3a)$$

while for a field applied along x<sub>1</sub>, Eq. (2) becomes

$$B_1 x_1^2 + B_2 x_2^2 + B_3 x_3^2 + 2r_{31}E_1 x_1 x_3 = 1. \quad (3b)$$

Of the linear electro-optic coefficients appearing in Eqs. (3a) and (3b),  $r_{31}$  is the largest for KNbO<sub>3</sub>,  $105 \times 10^{-12}$  m/V.[5] Utilization of this strong effect requires that a TE guided mode propagating in the 5 direction (the shear direction between the x<sub>1</sub> and x<sub>3</sub> axes) in the crystal be used. The geometry of the proposed device is shown in Fig. 5.

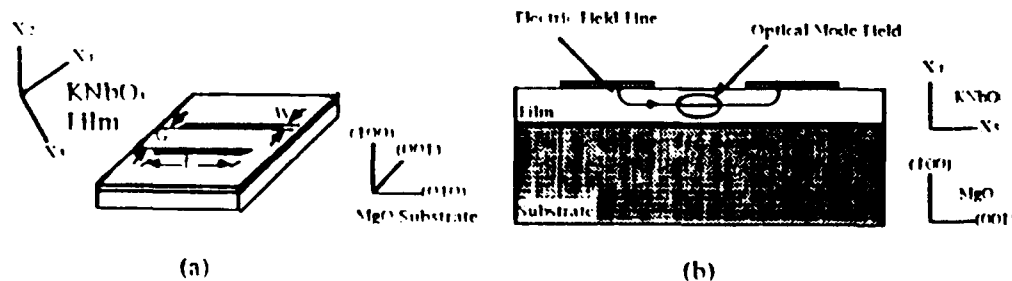


Fig. 5. Geometry of the proposed KNbO<sub>3</sub> electro-optic modulator.

The total phase shift for a TE mode propagating a distance  $L$  along the  $z$  direction in the film is  $\Delta\beta L = 2\pi L(\Delta n_5)/\lambda$ . From Eq. (3b),  $\Delta n_5$  can be found to be

$$\Delta n_5 = -\frac{1}{2} n_5^3 r_5 E_1 \quad (4)$$

To determine the applied electric field,  $E$  must be determined for the electrode geometry shown in Fig. 7-1(b). The electrode geometry shown, where the horizontal field is used for modulation, has been studied in depth by several researchers[6,7,8,9], with the result that  $E_1$  in Eq. (4) can be replaced by  $\Gamma V/\sqrt{2} G$  where  $V$  is the applied voltage,  $G$  is the gap between the strip electrodes and  $\Gamma$  represents the overlap integral between the electrical and optical fields. The expression is modified by  $1/\sqrt{2}$  to determine the component of the total field in the  $x_1$  direction. The overlap integral can be calculated from

$$\Gamma = \left(\frac{\pi}{2}\right) \iint E |E'|^2 dA \quad (5)$$

where  $E$  is the applied electric field and  $E'$  is the normalized optical field distribution. Using Eqs. (4) and (5), the total phase shift can be written as

$$\Delta\beta L = -\frac{\pi}{2} n_5^3 r_5 \Gamma \left(\frac{V}{G}\right) \left(\frac{1}{\lambda}\right) \quad (6)$$

Device length and modulation voltage are two critical parameters in device design. For device optimization the product  $VL$  should be minimized. Equation (6) can be rewritten to identify the relationship between the other device parameters and the  $VL$  product. The result, using  $\pi$  as the desired phase shift for the modulator, is

$$VL = \frac{\sqrt{2} \lambda G}{n_5^3 r_5 \Gamma} \quad (7)$$

For minimization of  $VL$ ,  $(G/\Gamma)$  must be minimized. However,  $\Gamma$  is a function of  $G$  and the optical mode size. Alfness[6] and Marcuse[7] have graphically presented this relationship for use in device design.

Before choosing actual device dimensions, modulation bandwidth must be considered. The modulation bandwidth when determined from the lumped electrode parameters is dependent on the electrode design and the dielectric constant of the thin film. The bandwidth is determined from  $\Delta f = 1/\pi RC$  where  $R$  is the impedance of the device, typically  $50 \Omega$  (matched to the driving circuit), and  $C$  is the capacitance of the strip electrodes. For symmetric strip electrodes as shown in Fig. 5, the capacitance per unit length is[6,10]

$$\frac{C}{L} = \epsilon_{eff} \frac{K'(r_s)}{K(r_s)} \quad (8)$$

where  $r_s = (2W/G+1)^{-1}$  and  $\epsilon_{eff} = (\epsilon_0/2)(1+\epsilon_s)$  is the RF dielectric constant. For  $\text{KNbO}_3$  in the geometry considered here,  $\epsilon_s = \epsilon_5 = 74$ .  $K$  is the complete elliptic integral of the first kind and  $K'(r_s) = K[(1-r_s^2)^{1/2}]$ . Alfness[6] has graphically determined  $C/L$  and  $\Delta f \cdot L$  vs.  $G/W$  for  $\text{LiNbO}_3$  and the results can be scaled appropriately for  $\text{KNbO}_3$ .

Modulation bandwidth can also be limited by the inverse of the optical or electrical transit times. Normally, the bandwidth is limited by the electrodes and is determined as above. The bandwidth is therefore dependent on  $G/W$ , increasing as the ratio of  $G/W$  increases. However, from Eq. (7) it can be seen that a small electrode gap is required to minimize the  $VL$  product.

Therefore, to maximize the modulation bandwidth requires a small electrode width. The electrical transit time cutoff frequency places a practical limit on the electrode gap to width ratio. Calculated as

$$f_t = \frac{c}{\pi(r_g l)^{1/2}} \quad (9)$$

the cutoff frequency for  $\text{KNbO}_3$  is 1.5 GHz·cm and 2.2 GHz·cm for  $\text{LiNbO}_3$ . There is thus no advantage for  $G/W > 3$  for a  $\text{KNbO}_3$  device.

The ratio of drive voltage to modulation bandwidth can be used as a figure of merit in evaluating device design. Using Eqs. (7) and (8) presented above, the ratio is

$$V/N = \sqrt{2} \pi R \lambda \left( \frac{1}{n_o^2 r_{31}} \right) (G/L) (C/L) \quad (10)$$

Table 1 summarizes the device geometry and operation parameters for optimized modulators based on potassium niobate thin films and X-cut, Y-propagating titanium-diffused lithium niobate waveguides. Based upon the drive voltage to modulation bandwidth ratio and the V·L product, the potassium niobate based modulator compares favorably with the lithium niobate modulator. The potassium niobate modulator uses a much larger electro-optic coefficient than the lithium niobate modulator, but the advantage gained is partially offset by the larger dielectric constant of  $\text{KNbO}_3$  for the geometry considered. Based on the drive voltage to modulation bandwidth ratio, the theoretical potassium niobate modulator represents an 80% improvement over the lithium niobate modulator.

Table 1. Comparison of optimized phase modulators.

	$\text{KNbO}_3$ Thin Film	Ti-diffused $\text{LiNbO}_3$
Electro-optic Coefficient	$r_{31} = 105 \times 10^{-12} \text{ m/V}$	$r_{33} = 30.8 \times 10^{-12} \text{ m/V}$
RF Dielectric Constant, $\epsilon_s$	74	35
Electrode Gap, $G$ , (mm)	2	1
Electrode Width, $W$ , (mm)	1	2
Wavelength, $\lambda$ , (nm)	633	633
Overlap Integral, $\Gamma$	0.7	0.3
V·L Product, (V·mm)	2.2	6.4
Electrical Cutoff Freq., $f_t$ , (GHz·cm)	1.5	2.2
RC Bandwidth·Length, $\Delta f_{RC} \cdot L$ , (GHz·cm)	1.4	2.1
$(V/\Delta f)_{\min}$ , (V/GHz)	0.2	0.5

Very high quality lithium niobate devices are currently being produced. However, a large market for these devices has yet to develop. One of the principle reasons for the small market is the difficulty in integrating these devices with thin film optoelectronic technology. It is in this area that thin films such as potassium niobate can excel. Several very important materials issues need to be addressed before the thin films can take the place of the bulk single crystal devices, however. High optical losses continue to plague thin film waveguides. These losses, primarily due to scattering, must be decreased to acceptable levels based upon the device being considered. In addition, for best use of the thin film materials, they must be grown on silicon or gallium arsenide. Due to the high indices of refraction of Si and GaAs, low index ( $<2$ ) buffer layers must first be grown on the substrates before the electro-optic material. These buffer layers must possess a lattice suitable to match both the substrate and the electro-optic material. Work is currently in progress at North Carolina State University to grow such materials.

## SUMMARY

The refractive indices of epitaxial potassium niobate (001) thin films deposited on single crystal magnesium oxide (001) have been measured using a prism coupler. The films were fabricated using an ion beam sputter-deposition system and their compositions determined from Rutherford Backscattering spectra. The thickness of the films was in the range of 2000 to 2500 Å so the films supported only one TE mode. Smooth, transparent films that were slightly potassium deficient had a refractive index of 2.28. This result falls within the expected range of 2.279 to 2.329 for bulk single crystal  $\text{KNbO}_3$  with the same orientation as the films.

A model of an electro-optic phase modulator was developed which optimizes the drive voltage and modulation bandwidth of the device. The model was based on the epitaxial  $\text{KNbO}_3$  films grown on  $\text{MgO}$  (001) using the ion beam sputter-deposition technique. The characteristics of the optimized device demonstrate the potential of  $\text{KNbO}_3$  films to surpass bulk single crystal  $\text{LiNbO}_3$ , which is currently the material of choice for guided-wave integrated optics devices.

## ACKNOWLEDGEMENTS

The authors would like to acknowledge the support of the Office of Naval Research for its support of this research program, Dr. O. Auciello, Dr. K. J. Bachmann, and Dr. S. H. Rou for useful discussions contributing to this work, and the National Defense Science and Engineering Graduate Fellowship program for their support of T. M. Graettinger.

- <sup>1</sup>A. I. Kingon, S. H. Rou, M. S. Ameen, T. M. Graettinger, K. Gifford, O. Auciello, and A. R. Krauss, in *Ceramic Transactions*, vol. 14: Electrooptics and Non-Linear Optic Materials, edited by A. S. Bhalla, E. M. Vogel, and K. M. Nair (American Ceramic Society, Westerville, Ohio, 1990), pp. 179-196.
- <sup>2</sup>P. K. Tien and R. Ulrich, *J. Opt. Soc. Am.* **60**(10), 1325-1337 (1970).
- <sup>3</sup>R. Ulrich and R. Torge, *Applied Optics* **12**(12), 2901-2908 (1973).
- <sup>4</sup>I. P. Kaminow, An Introduction to Electrooptic Devices, (Academic Press, New York, 1974), p. 25.
- <sup>5</sup>Landolt-Bornstein, New Series, Group III (Springer, New York, 1981), Vol. 16, pt. A.
- <sup>6</sup>R. C. Alferness, *IEEE Trans. Microwave Theory Tech.*, **MTT-23**, 1121-1137 (1982).
- <sup>7</sup>D. Marcuse, *IEEE J. Quantum Electron.*, **QE-18**, 393-398 (1982).
- <sup>8</sup>D. Marcuse, (corrections to ref. 4), *IEEE J. Quantum Electron.*, **QE-18**, 807 (1982).
- <sup>9</sup>O. G. Ramer, *IEEE J. Quantum Electron.*, **QE-18**, 386-392 (1982).
- <sup>10</sup>J. S. Wei, *IEEE J. Quantum Electron.*, **QE-13**, 152-158 (1977).

## **Appendix 2**

# ION-BEAM REACTIVE SPUTTER DEPOSITION OF MgO THIN FILMS ON SILICON AND SAPPHIRE SUBSTRATES

ALICE F. CHOW, SHANG HSIEH ROU, DANIEL J. LICHTENWALNER, ORLANDO AUCIELLO\*, and ANGUS I. KINGON, NORTH CAROLINA STATE UNIVERSITY, RALEIGH, NC; \*also MICROELECTRONICS CENTER OF NORTH CAROLINA, RESEARCH TRIANGLE PARK, NC

## ABSTRACT

MgO thin films were deposited on silicon and sapphire substrates using ion-beam reactive sputtering. Films have been analyzed using x-ray diffraction, transmission electron microscopy, and atomic force microscopy. Highly oriented (100) MgO films have been obtained on Si (100) substrates. The in-plane orientation is predominantly  $[100]_{\text{MgO}} // [100]_{\text{Si}}$ , although a twist of up to  $\pm 10^\circ$  between grains is observed. Epitaxial films of MgO were deposited on four different orientations of sapphire. The MgO film orientation was (111) on c-cut (0001)  $\text{Al}_2\text{O}_3$  and exhibited double positioning boundaries in TEM analysis. On r-cut ( $1\bar{1}02$ )  $\text{Al}_2\text{O}_3$ , the MgO appears to be oriented (730) with tilt and twist of  $\pm 2^\circ$  between the grains. Epitaxial MgO oriented (110) and (111) were obtained on m-cut ( $10\bar{1}0$ ) and a-cut ( $11\bar{2}0$ ) sapphire orientations, respectively. In-plane directions were extracted from TEM analysis on all the samples. Atomic force microscopy revealed fairly smooth MgO films on sapphire, varying from 0.35 nm average roughness for the MgO film on the m-cut substrate to 0.80 nm on the r-cut substrate.

## I. INTRODUCTION

The integration of novel superconducting, electro-optic, and ferroelectric thin film devices with existing semiconductor processing technology requires the deposition of thin films of  $\text{YBa}_2\text{Cu}_3\text{O}_{7-x}$  (YBCO),  $\text{Pb}(\text{Zr}_x\text{Ti}_{1-x})\text{O}_3$  (PZT), or  $\text{KNbO}_3$  on substrates such as silicon and sapphire. Silicon is ubiquitously used and its processing technology is well understood. Sapphire exhibits many desired attributes for microwave applications, such as low loss and low dielectric constant, large substrate availability at low cost, and good mechanical strength [1].

While the scientific importance of YBCO, PZT, and  $\text{KNbO}_3$  on silicon or sapphire are evident, processing difficulties have hindered progress in this area. Buffer layers must be introduced to prevent interfacial reactions and diffusion between layers. For many applications, potential buffer layers must be epitaxially deposited on the substrate and be a good host lattice for the overlayer, as well as being chemically inert with the substrate and overlayers. A few candidates for buffer layers are YSZ and  $\text{CeO}_2$  [2]. Here we have chosen MgO because it has a low dielectric constant, good thermodynamic stability, chemical compatibility with many materials, and provides an acceptable lattice match for the multicomponent oxide films mentioned above.

The properties of YBCO,  $\text{KNbO}_3$ , and PZT are known to be dependent on crystalline orientation. For instance, c-axis YBCO results in the optimal  $J_c$  and  $T_c$  values, and thus a (100) oriented epitaxial MgO underlayer is desired for deposition of c-axis YBCO films. The electro-optic properties of  $\text{KNbO}_3$  thin films and the ferroelectric properties of PZT thin films as a function of crystalline orientation have not been thoroughly studied. Our goals in this work are two-fold: 1) to obtain epitaxial MgO films on silicon and sapphire substrates; and 2) to achieve various orientations of MgO films to enable further study of  $\text{KNbO}_3$  and PZT properties as a function of film orientation.

## II. EXPERIMENT

Ion-beam reactive sputtering was used to deposit the MgO films examined in this study. The deposition system has been described in detail elsewhere [3]. Briefly, the system is pumped using a 330 l/s turbomolecular pump, attaining a background pressure in the mid  $10^{-7}$  torr range. A 3-cm diameter Kaufman-type ion source is used to sputter a 12.5 cm diameter magnesium metal target. A 500eV, 20mA  $\text{Xe}^+$  ion beam was used, with  $\text{O}_2$  gas added to the chamber

serving as the reactive species. Substrates were mounted to a radiatively heated substrate block using silver paste. Substrate thermocouple temperatures were calibrated using an optical pyrometer to measure a Si substrate, and comparing it to the melting point of an Al bead mounted nearby.

We used acetone, methanol, and deionized water for cleaning both silicon and sapphire substrates. Because silicon readily oxidizes and the amorphous silicon oxide may disrupt the epitaxial correlation of silicon with the arriving film atoms, passivation of the surface is required. A buffered hydrogen fluoride (BOE) dip etch was used to achieve a hydrogen terminated silicon surface [4].

After the substrates are mounted, heated to the desired temperature at approximately  $10^{\circ}\text{C}/\text{minute}$ , and chamber pressure minimized, we presputtered the magnesium target while the substrates were shuttered. While the sapphire substrates are insensitive to an oxygen environment, silicon must be especially guarded from an oxygen background to prevent silicon oxide formation. Therefore, for deposition on silicon, the magnesium was presputtered with no oxygen added. After opening the shutter and depositing  $\sim 10\text{\AA}$  of material,  $0.5\text{ sccm}$  of oxygen flow ( $1.2 \times 10^{-4}\text{ torr}$ ) was initiated, resulting in reactive sputtering of  $\text{MgO}$ . A substrate temperature of  $500^{\circ}\text{C}$  was used. For sapphire, a steady oxygen pressure was established before the run. An oxygen flow of  $0.5\text{ sccm}$  was also used, and substrate temperatures ranged from  $500\text{--}700^{\circ}\text{C}$ . The establishment of  $0.5\text{ sccm}$  oxygen flow resulted from an earlier oxygen flow/deposition rate calibration to determine minimum oxygen flow required to have a magnesium oxide (reacted) target surface. Minimum oxygen flow was demanded due to the possibility of obstruction of oriented growth by the presence of too much oxygen [5].

X-ray diffraction (XRD), transmission electron microscopy (TEM), and atomic force microscopy (AFM) using a Digital Instruments Nanoscope II, were performed to characterize our samples. This provides a complete analysis of film orientation, microstructure, and surface morphology.

### III. RESULTS and DISCUSSION

X-ray diffraction was performed on all samples. The XRD results show oriented  $\text{MgO}(100)$  on  $\text{Si}(100)$ ,  $\text{MgO}(111)$  on  $\text{Al}_2\text{O}_3(0001)$ ,  $\text{MgO}(110)$  on  $\text{Al}_2\text{O}_3(1\bar{1}0)$ , and  $\text{MgO}(111)$  on  $\text{Al}_2\text{O}_3(1\bar{1}20)$ . These XRD patterns are shown in Fig. 1. The XRD results, although indicating oriented film growth, are not sufficient to confirm epitaxy. No  $\text{MgO}$  peaks were observed for films deposited on  $(1\bar{1}02)\text{Al}_2\text{O}_3$ .

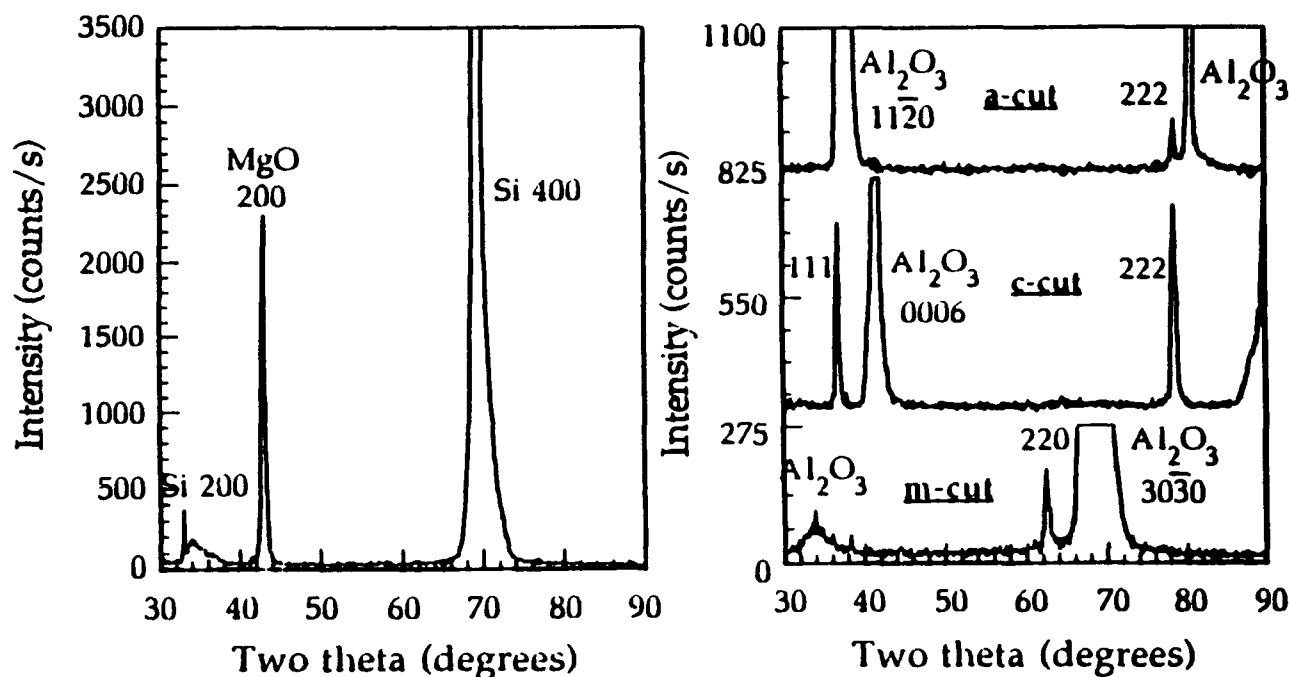


Fig. 1. X-ray diffraction patterns of  $\text{MgO}$  on silicon, and on a-cut, c-cut, and m-cut sapphire.

The MgO films on Si were further examined using both plan-view and cross-sectional TEM. A plan view micrograph and electron diffraction pattern are shown in Fig. 2. A large selected area aperture size was used to obtain the electron diffraction patterns from a reasonable large area. The diffraction pattern indicates that the (001) MgO in-plane orientation lies parallel to the (001)Si, although twisted up to  $\pm 10^\circ$  about the substrate normal. The twist is large enough to produce distinct grain boundaries in the MgO film. The grain size is about 300Å, as seen in the TEM micrograph (Fig. 2). These highly oriented MgO films would serve as suitable buffer layers for PZT films used as nonvolatile memories. Cross-sectional TEM has revealed that a thin (<15Å) amorphous layer is present at the MgO/Si interface. It has not been determined whether this layer forms before, during, or after deposition. Because of the non-UHV conditions of our chamber, it is possible that an oxide formed prior to deposition. The presence of a thin amorphous region on the substrate initially could explain the lack of complete epitaxy for the MgO film. Improving the Si passivation procedure may remedy this occurrence [6].

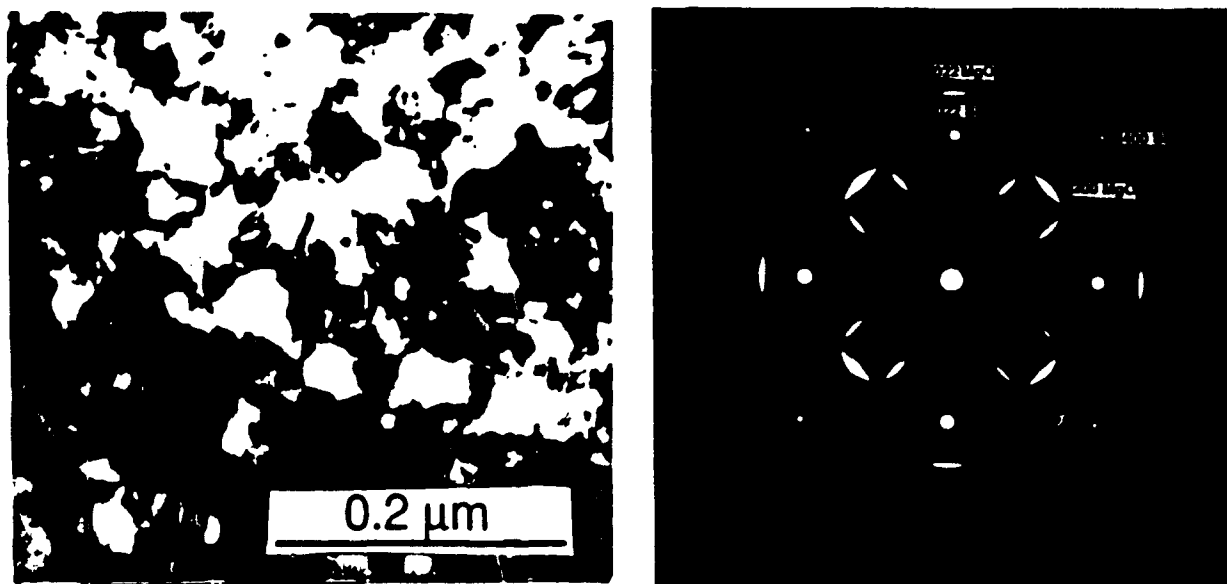


Fig. 2. Plan view micrograph and electron diffraction pattern of MgO film on (100) silicon.

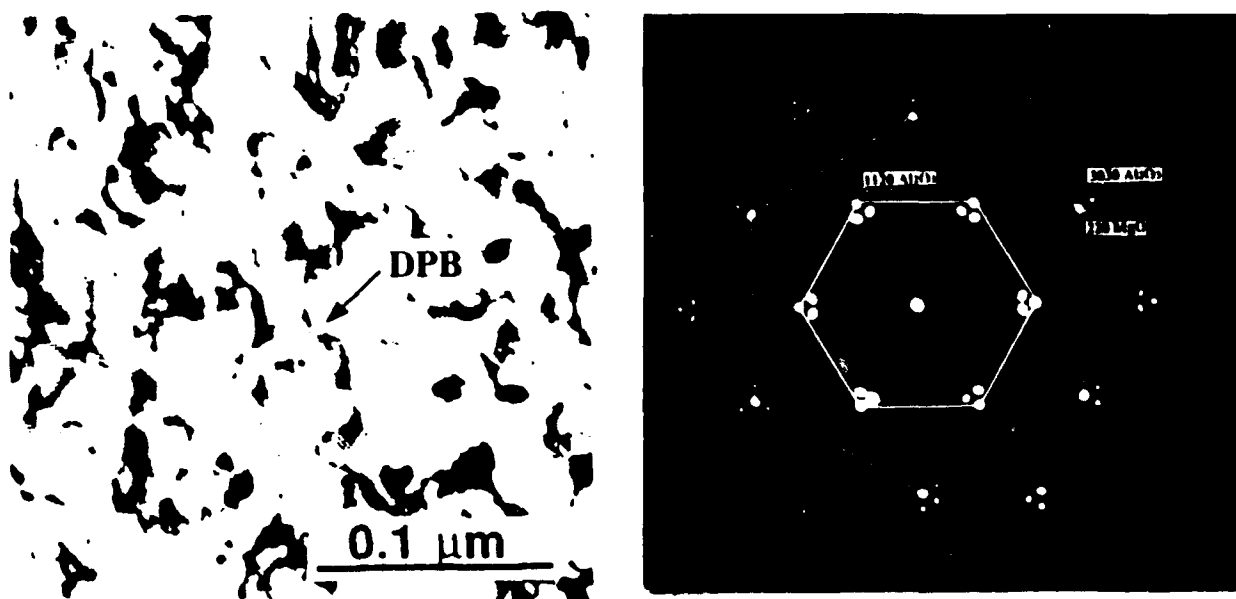


Fig. 3. Plan view micrograph and electron diffraction pattern of MgO on c-cut sapphire. The boundaries observed in the micrograph are double positioning boundaries.

All MgO films on sapphire exhibited epitaxial growth as revealed by the plan-view electron diffraction patterns. The MgO on c-cut (0001)Al<sub>2</sub>O<sub>3</sub> contained double positioning boundaries as shown by the micrograph in Fig. 3. Two energetically equivalent sets of nucleation sites are present, thus the arriving atoms have a choice of inhabitation resulting in grains separated by partial dislocation-like boundaries, or double positioning boundaries ( $\frac{1}{6}[\bar{2}11]$  lattice shifts). The electron diffraction pattern shows the in-plane epitaxial alignment  $[01\bar{1}]MgO//[10\bar{1}0]Al_2O_3$  and  $[\bar{2}11]MgO//[1\bar{2}\bar{1}0]Al_2O_3$ .

The r-cut(1 $\bar{1}$ 02) Al<sub>2</sub>O<sub>3</sub> sample revealed tilt and twists of  $\pm 2^\circ$  between the grains shown in Fig. 4. Low angle boundaries and dislocations were also identified. The electron diffraction pattern showed (100)MgO plane matching with (2 $\bar{2}$ 01)Al<sub>2</sub>O<sub>3</sub>. (The diffraction pattern shown was obtained by tilting the sample  $23^\circ$  from the r-plane, resulting in an epitaxial (100)MgO pattern.) This made the indexing difficult in TEM and the x-ray diffraction analysis unapplicable. We deduced from the electron diffraction pattern that a high index (730)MgO plane matched with r-cut(1 $\bar{1}$ 02) Al<sub>2</sub>O<sub>3</sub>. The in-plane orientations were  $[\bar{3}70]MgO//[1\bar{1}01]Al_2O_3$  and  $[001]MgO//[11\bar{2}0]Al_2O_3$ .

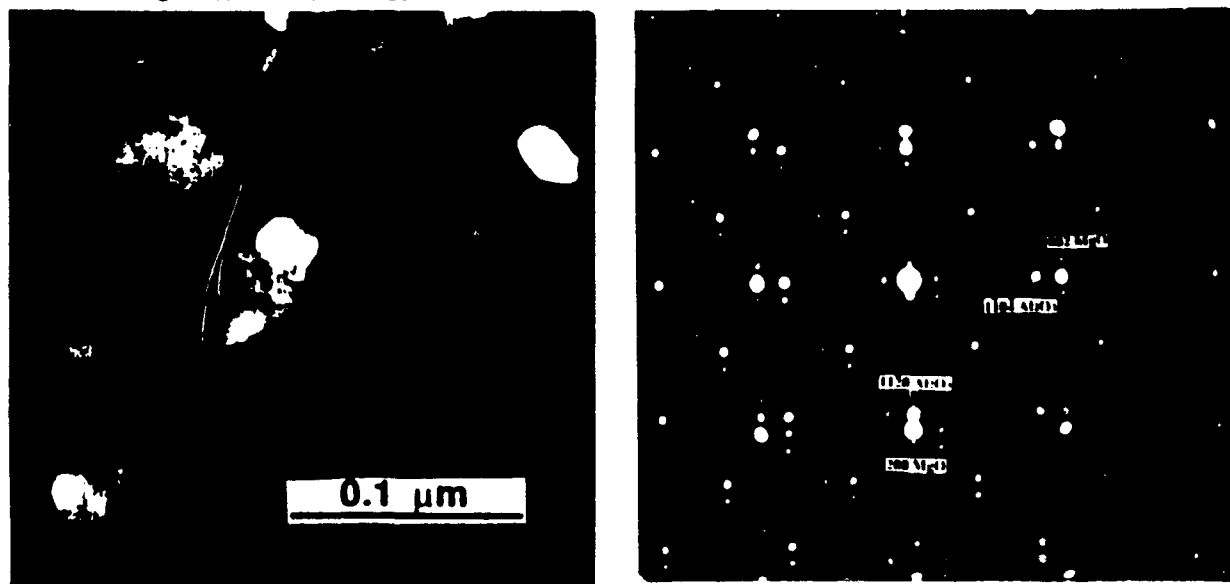


Fig. 4. Plan view micrograph and electron diffraction pattern of MgO on r-cut sapphire. The MgO is epitaxial with tilt and twists of  $\pm 2^\circ$  between the grains.

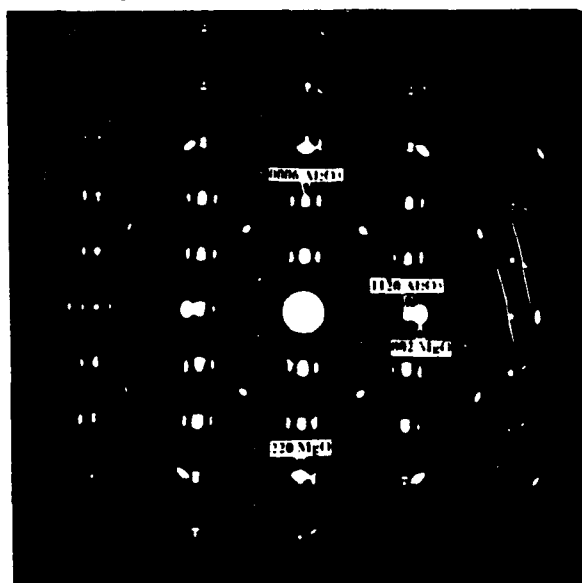


Fig. 5. Electron diffraction pattern of MgO on m-cut sapphire.

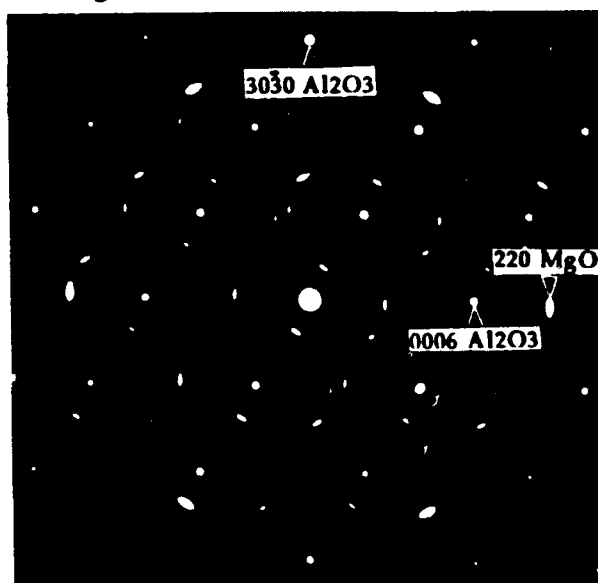


Fig. 6. Electron diffraction pattern of MgO on a-cut sapphire.

The microstructure of the MgO(110) on m-cut (10 $\bar{1}$ 0)Al<sub>2</sub>O<sub>3</sub> consists of low angle grain boundaries, tilt and twists of  $\pm 3^\circ$  between the grains, and dislocations due to the lattice mismatch. The electron diffraction pattern in Fig. 5 reveals in-plane orientations of [001]MgO//[1 $\bar{2}$ 10]Al<sub>2</sub>O<sub>3</sub> and [ $\bar{1}$ 10]MgO//[0001]Al<sub>2</sub>O<sub>3</sub>.

TEM analysis of the MgO(111) on a-cut (11 $\bar{2}$ 0)Al<sub>2</sub>O<sub>3</sub> revealed a microstructure also of low angle grain boundaries with tilt and twists of  $\pm 3^\circ$  between the grains. The in-plane orientations are [01 $\bar{1}$ ]MgO//[000 $\bar{1}$ ]Al<sub>2</sub>O<sub>3</sub> and [ $\bar{2}$ 11]MgO//[ $\bar{1}$ 100]Al<sub>2</sub>O<sub>3</sub> as determined by the electron diffraction pattern in Fig. 6.

The orientations of our MgO on sapphire match those reported by Talvacchio et al. [7], except for the MgO orientation on r-cut sapphire; they achieved MgO(100) on r-cut sapphire as determined by XRD and RHEED analysis. However, their film processing included post deposition annealing, while our films were deposited in situ, nor did they perform microstructural characterization on their MgO films.

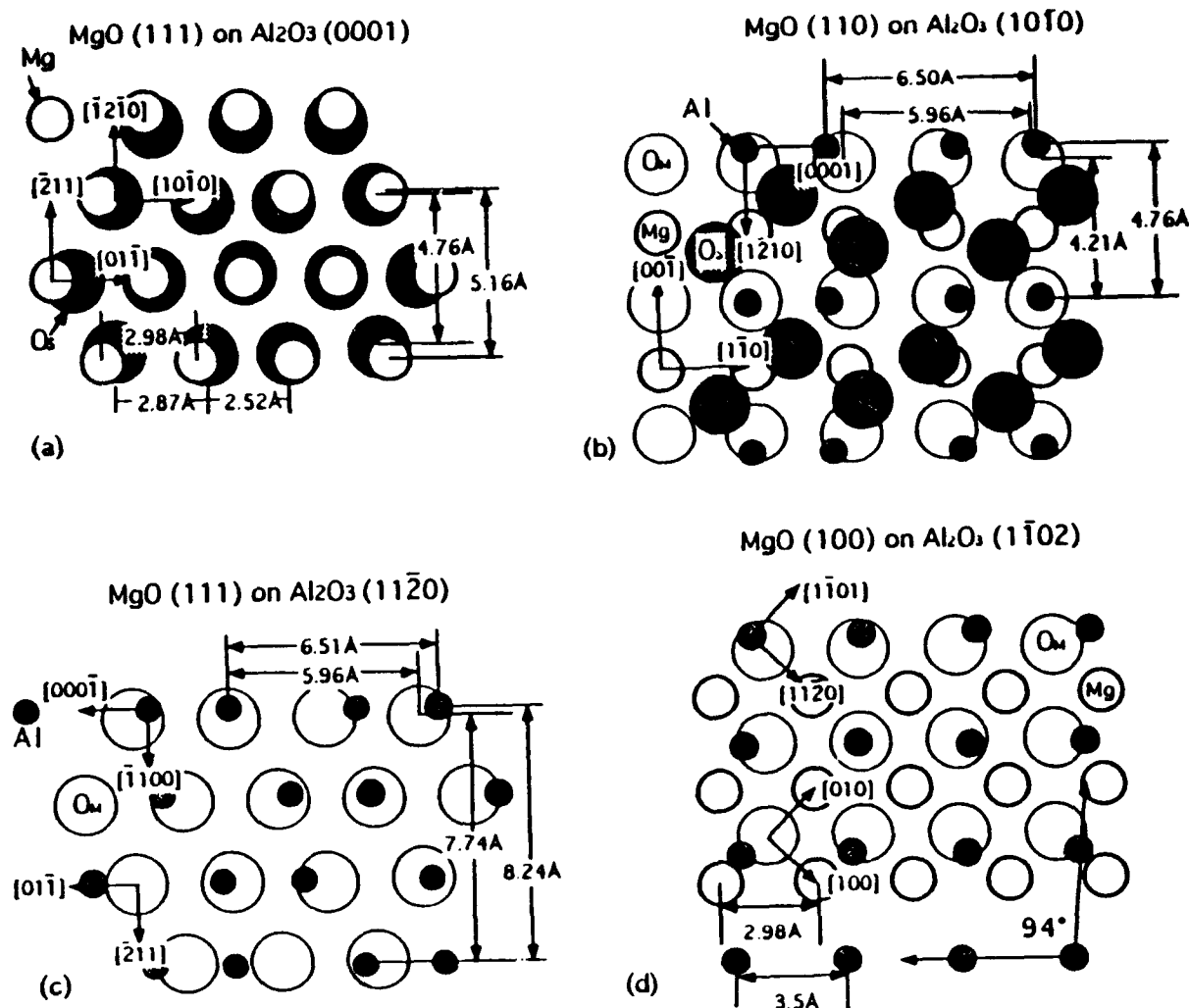


Fig. 7. Planar views of atomic orientations of MgO on various orientations of Al<sub>2</sub>O<sub>3</sub> as suggested from TEM electron diffraction patterns. These are shown for the purpose of visualizing lattice match and symmetry, not to imply the actual atomic positions of the Mg and O atoms bonded to sapphire; O<sub>S</sub>=Oxygen atom of sapphire, O<sub>M</sub>=Oxygen atom of MgO.

Lattice matching diagrams were constructed to better reveal the epitaxial relationships between the MgO and sapphire. The lattice mismatch between first neighbor atom-atom lengths were between 6-12%. Although this is an appreciable amount of mismatch, the epitaxial growth of the MgO and the symmetry correlation of the MgO with  $\text{Al}_2\text{O}_3$  suggest that structural symmetry is a more important factor here in determining orientation than simply lattice mismatch. For the c-cut and a-cut sapphire, the surface comprised of planes of either all aluminum or all oxygen as depicted in Figs. 7(a) and 7(c) which would explain the matching of the close-packed (111)MgO plane which also contains all oxygen or magnesium atoms. Whereas, in the case of m-cut and r-cut, the surface consists of a mixture of aluminum and oxygen atoms seen in Fig. 5(b) and 5(d). For the MgO on r-cut sapphire schematic, although the oxygen atoms of the MgO match symmetrically reasonably well with the array of the Al atoms in the r-plane (although with 15% mismatch), the Al atoms are arranged in a distorted array, having a  $94^\circ$  angle between atoms. This distorted Al array, plus the large lattice mismatch, is expected to be the cause of the MgO being tilted away from the (100) orientation in our films, as well as for those reported by Berezin et al. [5].

Atomic force microscopy (AFM) revealed smooth texture for the MgO films on sapphire. The MgO film deposited at  $700^\circ\text{C}$  on m-cut (10 $\bar{1}$ 0)  $\text{Al}_2\text{O}_3$  measured over 1000 nm distance displayed an average surface roughness,  $R_a$ , of 0.35 nm. Also deposited at  $700^\circ\text{C}$ , the film on c-cut (0001)  $\text{Al}_2\text{O}_3$  displayed an  $R_a$  of 0.53 nm. For the MgO on r-cut (1102)  $\text{Al}_2\text{O}_3$ , the film was a bit rougher with the  $R_a = 0.80$  nm. That particular sample was deposited at  $500^\circ\text{C}$  which may have contributed to producing a rougher surface, along with the film growth orientation.

## V. CONCLUSIONS

Highly oriented MgO(100) films on Si(100) and epitaxial MgO films on  $\text{Al}_2\text{O}_3$  were deposited using ion-beam reactive sputtering. The orientation and microstructure of the MgO films on  $\text{Al}_2\text{O}_3$  are controlled by the  $\text{Al}_2\text{O}_3$  orientation. Analysis of the surface smoothness using AFM revealed that the MgO films on  $\text{Al}_2\text{O}_3$  have average roughness of  $\sim 5\text{\AA}$ , which is extremely smooth.

Consequently, we may improve our results on silicon by producing better surface passivation. Effects of temperature and oxygen pressure variations on the orientation of MgO should be explored. Growth conditions and sapphire orientations resulting in (100)MgO on  $\text{Al}_2\text{O}_3$  need to be addressed further. Large area substrate deposition and overlayer deposition of YBCO, PZT, and  $\text{KNbO}_3$ , along with studies of orientation-dependent properties will be attempted as well.

## V. ACKNOWLEDGEMENTS

We acknowledge support from the Office of Naval Research under contract N00014-91-J-1307 and from the National Science Foundation under grant DMR-88-07367.

## VI. REFERENCES

1. X.D. Wu, R.E. Muenchausen, N.S. Nogar, A. Pique, R. Edwards, B. Wilkens, T.S. Ravi, D.M. Hwang, and C.Y. Chen, Appl. Phys. Lett. 58, 304, (1991).
2. T. Inoue, T. Ohsuna, L. Luo, X.D. Wu, C.J. Maggiore, Y. Yamamoto, Y. Sakurai, and J.H. Chang, Appl. Phys. Lett. 59, 3604, (1991).
3. D.J. Lichtenwalner, O. Auciello, R.R. Woolcott Jr., C.N. Soble II, to be published in J. Vac. Sci. Tech. A 10, July/Aug. (1992).
4. G.S. Higashi, R.S. Becker, Y.J. Chabal, and A.J. Becker, Appl. Phys. Lett. 58, 15, (1991).
5. A.B. Berezin, C.W. Yuan, A.L. de Lozanne, S.M. Garrison, and R.W. Barton, IEEE Trans. Magnetics 27, 970, (1991).
6. D.B. Fenner, D.K. Biegelsen, and R.D. Bringans, J. Appl. Phys. 66, 419, (1989).
7. J. Talvacchio, G.R. Wagner, and H.C. Pohl, Physica C 162-164 (1989) 659-60.

## **Appendix 3**

# GROWTH, MICROSTRUCTURES AND OPTICAL PROPERTIES OF KNbO<sub>3</sub> THIN FILMS

THOMAS M. GRAETTINGER\*, P. A. MORRIS\*\*, R. R. WOOLCOTT\*,  
F. C. ZUMSTEG\*\*, A. F. CHOW\*, AND A. I. KINGON\*

\*North Carolina State University, 1001 Capability Dr., Raleigh, NC 27695-7919

\*\*DuPont Company, Experimental Station, Wilmington, DE 19880-0356

## ABSTRACT

Potassium niobate, KNbO<sub>3</sub>, possesses high nonlinear optical coefficients making it a promising material for frequency conversion into the visible wavelength range. While epitaxial thin films of KNbO<sub>3</sub> have been reported [1,2], only limited data exists concerning the optical loss mechanisms and nonlinear optical properties of these films. In this study, epitaxial thin films of KNbO<sub>3</sub> have been grown using ion beam sputter deposition and evaluated in terms of their microstructures and optical properties. Characterization of the microstructures of these films includes the in-plane epitaxial relationship to the substrate. The relationships between the growth parameters and microstructures developed to the indices of refraction and the optical losses (absorption and scattering) are discussed.

## INTRODUCTION

The next generation of laser writing and optical storage devices will require a high resolution coherent light source. The resolution necessary can be achieved by using a blue light source where high resolution is achieved because of the short wavelength. Currently no compact blue laser source is commercially available, but the production of blue laser radiation through second harmonic generation (SHG) in a nonlinear optical material presents the most promising approach demonstrated thus far. Achieving the necessary second harmonic power (1-5 mW) from a relatively low power semiconductor laser diode requires high conversion efficiency in the nonlinear material.

Many factors influence the SHG efficiency including the nonlinear susceptibility of the material ( $d_{ijk}$ ), the refractive index ( $n$ ), the optical pathlength ( $L$ ), and the waveguide width and thickness ( $w, t$ ) as shown in the following equation.

$$\frac{P(2\omega)}{P(\omega)} \propto \frac{d_{ijk}^2}{n^3} L^2 \frac{P(\omega)}{w \cdot t} \quad (1)$$

This relationship makes clear the advantages of using the nonlinear material in a resonator system where  $L$  becomes large enough to produce efficient SHG output. Such systems have been demonstrated for several materials including  $\text{KNbO}_3$ . [3,4] Also clear from the above relationship is the increased efficiency resulting from confining the fundamental beam,  $P(\omega)$ , in a waveguide structure, thereby decreasing the parameter  $t$ .

The nonlinear optical material used determines the device design. Many of the commonly used nonlinear materials including KTP,  $\text{LiTaO}_3$ , and  $\text{LiNbO}_3$  require complex phase matching schemes in order to produce efficient SHG. [5,6,7]  $\text{KNbO}_3$ , however, can be used to produce light in the blue region of the optical spectrum by Type I phase matching. [8] This is an attractive attribute for a thin film device where producing complex phase matching structures within the material may be difficult. In addition,  $\text{KNbO}_3$  possesses large nonlinear optical susceptibilities, comparable to the other materials mentioned.  $\text{KNbO}_3$  thin films have been fabricated by several growth methods including ion beam sputtering [1], rf-diode sputtering [2], the sol-gel process [9], and liquid phase epitaxy, LPE [10]. To date, the films produced by the sputtering methods have exhibited the best optical properties with optical propagation losses as low as 1.1 dB/cm reported [2].

Low optical propagation losses are paramount to fabricating a viable SHG device. Two primary loss mechanisms exist for transmission through waveguides, absorption and scattering. Absorption can result from impurities, carriers, and interband transitions. Absorption decreases SHG efficiency by the following,

$$\frac{P(2\omega)}{P(\omega)} \propto \frac{d_{ijk}^2}{n^2} \frac{1}{\kappa} P(\omega) \quad (2)$$

where  $\kappa$  is the absorption coefficient of the nonlinear optical material. While absorption processes have been shown to limit the properties of several optical materials, scattering is the major component of the propagation loss in most thin film waveguides. Scattering is typically caused by inhomogeneities in the film, microstructural defects, and imperfections at the film-substrate and film-surface interfaces. The loss produced by interface roughness is a good example to illustrate the interface control necessary to produce a low-loss thin film. The radiation loss factor,  $\alpha$ , is related to the interface roughness by [11]

$$2\alpha \propto \frac{(n_f^2 - n_s^2)b^2}{t^3} \quad (3)$$

where  $n_f$  is the refractive index of the film,  $n_s$  is the index of the substrate,  $b$  is the amplitude of the interface roughness, and  $t$  is the film thickness as shown in Fig. 1. Loss due to interface roughness is especially difficult to control for nonlinear optical materials which have high indices of refraction,  $n > 2.00$ . The large index difference between the light guiding film layer and the substrate

scales the radiation loss factor by the difference of the squares of the indices, making even small interface roughness result in large optical propagation loss for thin films.

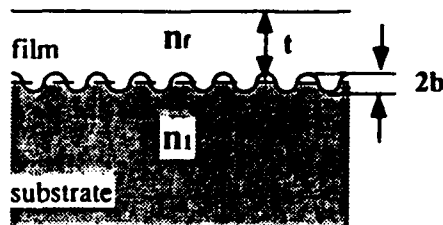


Fig. 1. Model used to calculate the radiation loss caused by interface roughness.

The microstructural requirements for low-loss light-guiding thin films are not well defined. Microstructural features such as high and low angle grain boundaries, grain size, and domain walls may contribute to large propagation loss through scattering. The detriment to film quality of each feature is expected to be related to the material-substrate system chosen. Control of film microstructure is possible by proper choice of growth technique and deposition parameters.

#### KNbO<sub>3</sub> FILM GROWTH

KNbO<sub>3</sub> films have been grown by rf-diode sputtering, LPE, sol-gel, and ion beam sputtering as stated previously. In this investigation, KNbO<sub>3</sub> films were grown using two ion beam sputter deposition processes. The first, shown in Fig. 2, was developed at N. C. State [1]. This process uses a single primary ion source to sputter material from multiple, elemental and elemental oxide targets which are sequentially rotated in front of the ion beam. Thus, thin layers of the target materials, niobium and potassium superoxide (KO<sub>2</sub>), are deposited on the substrate. At the deposition temperature, these layers are continuously interdiffusing and the proper structure is formed in situ. Control of film stoichiometry is achieved by adjusting the relative thickness of the layers. The thickness of each layer is computer-controlled through feedback from a quartz crystal resonator.

A second ion beam sputter deposition system, shown in Fig. 3, has recently been set up at DuPont. This system uses two primary ion sources to cosputter the Nb and KO<sub>2</sub> targets. Stoichiometric control is attained by adjusting the relative sputtering rates of the two targets. The sputtering rates are primarily controlled by adjusting the ion beam energy and ion beam current incident on each target. In addition, the deposition rate from each target is monitored by a quartz crystal resonator.

Many process parameters were kept constant in both deposition systems so that changes in nucleation and growth mechanisms resulting from cosputtering versus layer by layer growth could be investigated. Table I summarizes the most important common processing conditions. Single crystal, (001) oriented magnesium oxide, MgO, was used as the substrate for all films in this study. The substrate temperature during deposition was between 600 and 650°C with the higher temperatures used during the growth of thick films for optical characterization. The ion beam energy was kept in the range of 500 to 1000 eV to minimize damage to the growing film from high energy backscattered primary ions. Films from 500 to 5000 Å were deposited using both deposition techniques.

Table I. Process parameters for ion beam sputter deposited KNbO<sub>3</sub> thin films.

Targets	Nb, KO <sub>2</sub>
Substrate	MgO (001)
Growth Temp.	600-650°C
Ion beam energy	500-1000 eV
Ion beam current	0.025-0.100 mA/cm <sup>2</sup>
Growth rate	500 Å/hr.
Oxygen background pressure	1x10 <sup>-5</sup> -1x10 <sup>-4</sup> torr
Cooling rate	5°C/min.

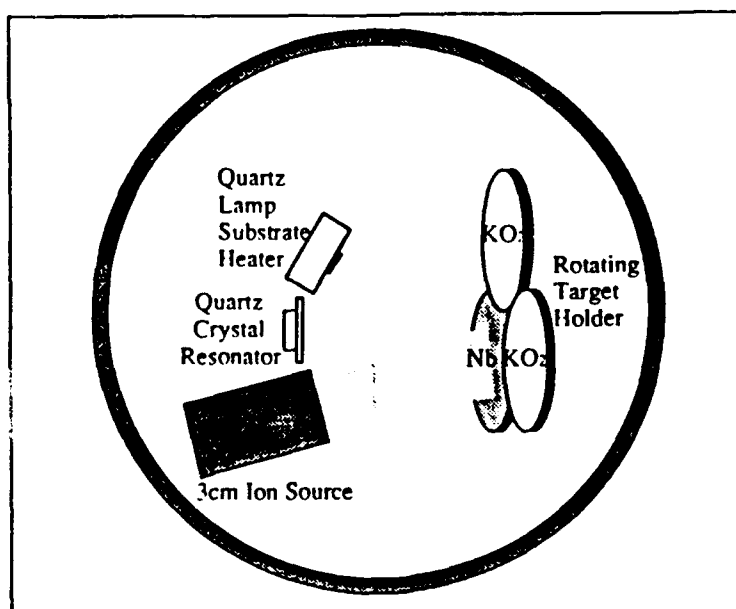


Fig. 2. Ion beam sputter deposition system used for layer-by layer growth.

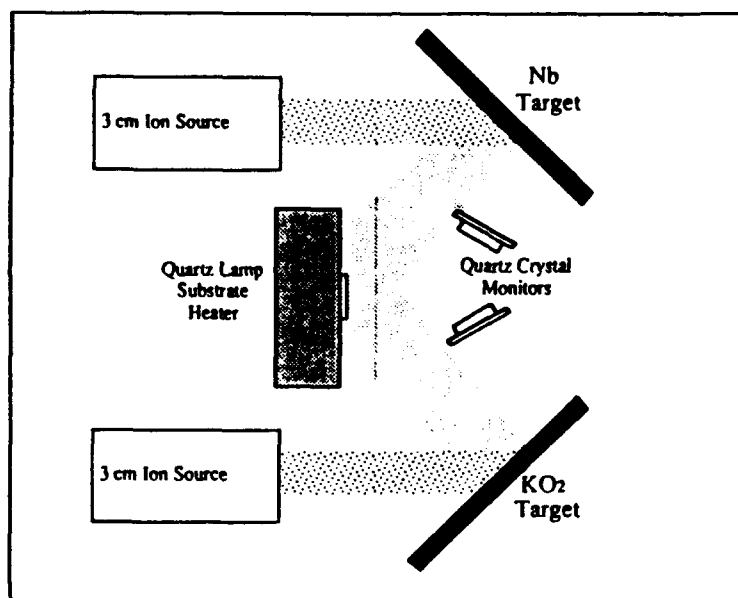


Fig. 3. Ion beam sputter deposition system used for cosputtering.

Rutherford Backscattering Spectrometry (RBS) was used to determine film composition. A 2 MeV  $^4\text{He}^+$  ion beam normally incident on the samples was used for the measurements. Fig. 4 shows the result of a typical RBS measurement. The experimental spectrum shown is in excellent agreement with the simulated spectrum of a stoichiometric  $\text{KNbO}_3$  film also shown in the figure. Simulated RBS spectra were also used to determine the thickness of films which supported only single guided modes. DekTak measurements were used to verify the thickness determined by RBS. The thickness determined was then used to calculate the refractive index of such films.

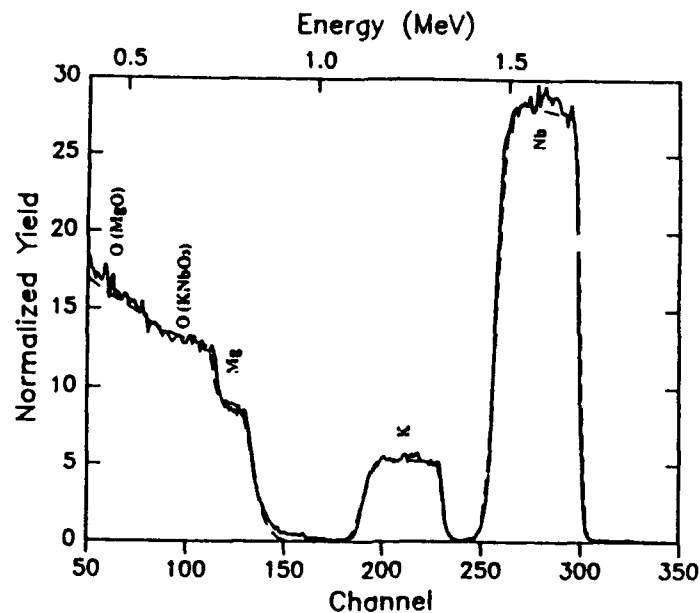


Fig. 4. RBS spectrum of a  $\text{KNbO}_3$  thin film grown on  $\text{MgO}$ . The dashed line represents the simulated spectrum of a stoichiometric  $\text{KNbO}_3$  film.

#### EPITAXY STUDY

Crystal orientation is critically important to SHG performance. Phase matching of the fundamental and second harmonic waves can normally be accomplished only in certain crystallographic directions in a crystal. Therefore, it is desirable to produce a thin film that is a single crystal, requiring epitaxy in both planar directions of the thin film and no microstructural defects. In practice it is very difficult to grow a true heteroepitaxial film. Lattice mismatch between film and substrate is often accommodated by the formation of microstructural defects such as high and low-angle grain boundaries and the formation of domain walls in ferroelectric thin films. For these reasons, neighboring grains or domains may not have the same crystallographic orientation across the boundary or wall, ruining the phase matching conditions as the fundamental and second harmonic waves cross these boundaries.

The standard x-ray diffractometer theta-two theta scan is a powerful technique for determining the crystalline structure of thin films and for determining if any preferential orientation exists. The resulting pattern is also useful in identifying the crystalline phases present. Fig. 5 shows a typical x-ray diffraction pattern for a  $\text{KNbO}_3$  thin film deposited on  $\text{MgO}$ . From this diffraction pattern it is clear that the film is single phase  $\text{KNbO}_3$  and highly

oriented with  $(110)\text{KNbO}_3\parallel(001)\text{MgO}$  where the indices given for  $\text{KNbO}_3$  are for the orthorhombic phase. This orientation of the orthorhombic unit cell is pictured in Fig. 6. As shown in the figure, the  $[001]\text{KNbO}_3$  is in the plane of the film. However, it can not be determined from the standard diffraction pattern if the  $[001]\text{KNbO}_3$  is parallel to the  $[100]\text{MgO}$  or the  $[010]\text{MgO}$ . The in-plane orientation of the film, is necessary for phase matching considerations as discussed earlier.

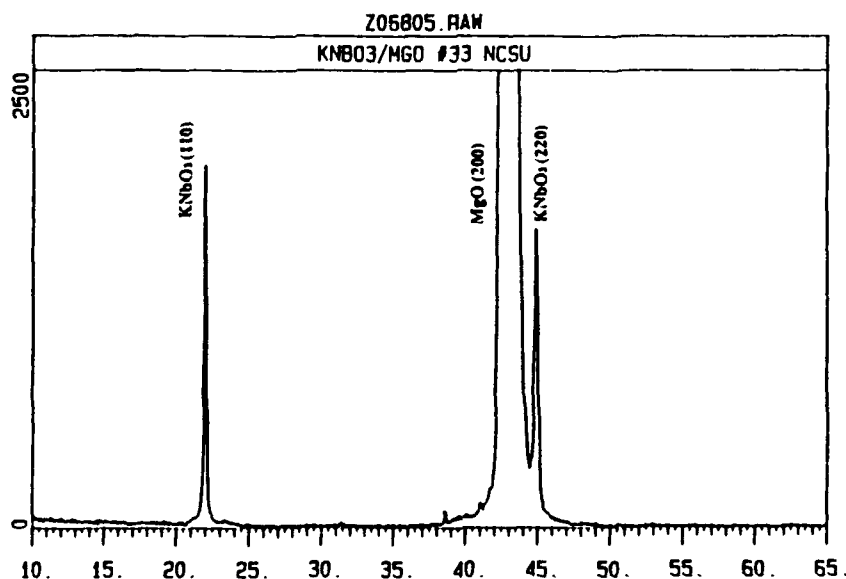


Fig. 5. X-ray diffraction pattern of a  $\text{KNbO}_3$  thin film deposited on  $\text{MgO}(001)$ .

In order to investigate the in-plane orientation of the  $\text{KNbO}_3$  thin films, a pole figure rotation stage in combination with an x-ray diffractometer was used. This apparatus has the ability to probe crystal planes which are not parallel to the substrate surface. First,  $(110)$  pole figures were constructed for the  $\text{KNbO}_3$  thin films and a representative figure is shown in Fig. 7. This figure makes it clear that the film is tilted along the  $\text{MgO}$   $[100]$ ,  $[010]$ ,  $[\bar{1}00]$ , and  $[0\bar{1}0]$  directions. Samples deposited by both ion beam sputtering methods exhibited this behavior, suggesting that the tilt is a substrate influenced characteristic and is not related to deposition method. Lattice tilt is a well known mechanism for accommodating lattice mismatch between film and substrate. The lattice mismatch between the  $(001)\text{KNbO}_3$  and  $[100]\text{MgO}$  planes is 6.0%. This mismatch is relatively large for achieving high quality heteroepitaxial growth. In addition to tilt, low angle grain boundaries twinning, and inversion domain

boundaries have been observed previously in  $\text{KNbO}_3$  thin films grown by ion beam sputtering.[12]

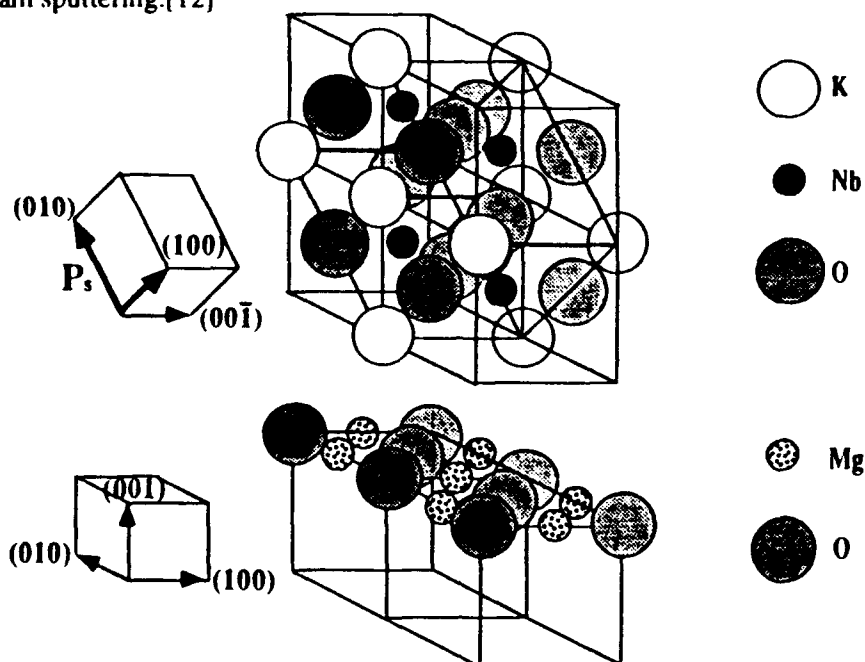


Fig. 6. The orientation of the orthorhombic unit cell of  $\text{KNbO}_3$  on  $\text{MgO}(001)$ .

With this knowledge it is probable that complete in-plane epitaxy has not been achieved. The films may be best described as textured with in-plane rotation.

Due to the large lattice mismatch between  $\text{KNbO}_3$  and  $\text{MgO}$  the films may be highly strained. Others have reported the growth of tetragonal  $\text{KNbO}_3$  films[2] which may be a result of strain in those films. The  $(110)$  and  $(220)$  reflections of orthorhombic  $\text{KNbO}_3$  match closely the peaks observed for the ion beam sputtered films grown in this study. To confirm that the films grown by ion beam sputtering were indeed orthorhombic, the pole figure rotation stage was used to rotate the samples so that planes which are not parallel to the substrate surface would reflect in the standard diffractometer geometry. In this manner, the  $(131)$  and  $(311)$  planes, among others, were identified and their d-spacings are consistent with orthorhombic  $\text{KNbO}_3$ . Further, these planes also exhibited tilt about the expected positions which were based on alignment of the  $[110]\text{KNbO}_3$  and  $[001]\text{MgO}$  directions.

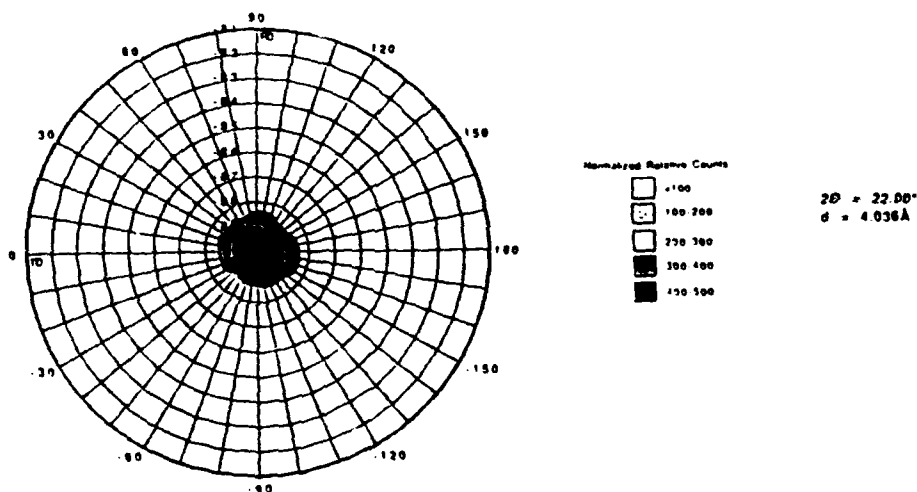


Fig. 7. (110) pole figure for a KNbO<sub>3</sub> thin film deposited on MgO.

## OPTICAL PROPERTIES

The indices of refraction of layer-by layer deposited and cosputtered KNbO<sub>3</sub> thin films were measured using the prism coupling m-line technique. The mode lines appeared relatively sharp as shown in Fig. 8 which shows the measurement of a layer-by layer deposited film. Both types of films supported TE and TM guided modes. The results of these measurements are presented in Table II along with the indices of bulk KNbO<sub>3</sub> for orientations which correspond to the guided modes. The film indices for TE modes should be compared to the (001) and (1  $\bar{1}$  0) indices of bulk KNbO<sub>3</sub>, 2.3291 and 2.2242, respectively, since these are the major and minor axes of the index ellipsoid in the plane of the film. If the films were single crystal, both values should have been observed as the films were rotated 90 degrees during the measurements. This birefringence was not observed, however. Instead, the measured TE indices match closely with the average of the bulk (001) and (1  $\bar{1}$  0) indices. The fact that birefringence was not seen in the TE measurements supports the conclusion that the films are textured with in-plane rotation as stated above. However, strain effects and twinning could also account for the lack of birefringence in the TE index. The TM indices of both types of ion beam sputtered films, on the other hand, are in good agreement with the expected (110) bulk index.

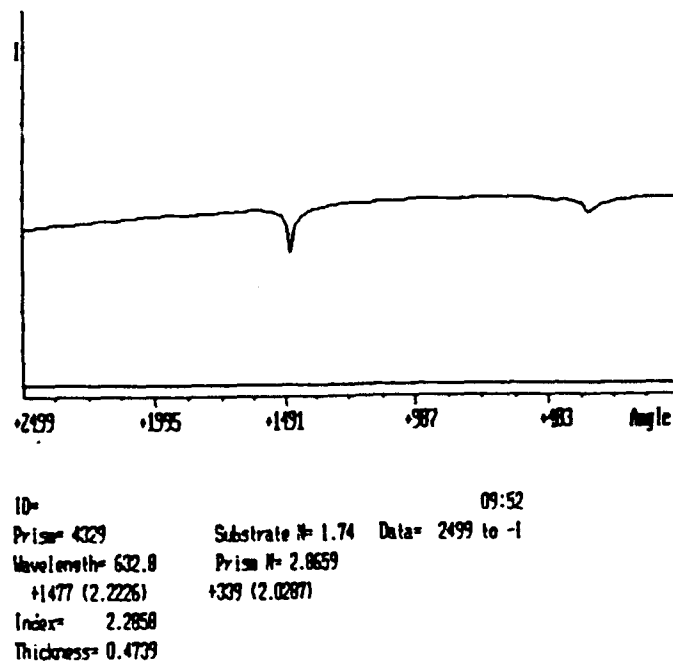


Fig. 8. Guided mode spectrum for an ion beam sputter deposited  $\text{KNbO}_3$  film.

Table II. Refractive indices of thin films and bulk  $\text{KNbO}_3$ .

Film	Substrate	Mode/Orientation	Refractive Index
Layer-by-layer	MgO	TE	$2.2856 \pm .0003$
		TM	$2.2021 \pm .0012$
Cosputtered	MgO	TE	$2.2207 \pm .0041$
		TM	$2.1975 \pm .0046$
Bulk $\text{KNbO}_3$		(001)	2.3291
		(110), (1 $\bar{1}$ 0)	2.2242

A fiber probe was used to measure the optical propagation loss in the  $\text{KNbO}_3$  films. A large degree of scattering prevented the measurement of propagation loss in the films using the fiber probe. As discussed earlier, microstructural features such as grain boundaries and interface roughness can be major contributors to scattering loss. These features are found in the sputtered films and must be controlled in the future to yield low-loss waveguides.

## SUMMARY

Thin films of  $\text{KNbO}_3$  were fabricated by ion beam sputtering using both layer-by-layer and cosputtering ion beam deposition methods. Both methods have demonstrated good compositional control and stoichiometric  $\text{KNbO}_3$  thin films have been produced. However, in-plane epitaxy is necessary to achieve efficient SHG in a thin film. To investigate the in-plane epitaxy of the films a pole figure rotation stage in combination with a standard x-ray diffractometer was used. The results of this study show that the  $\text{KNbO}_3$  films are tilted  $1\text{--}1.5^\circ$  about the substrate normal along the  $\text{MgO}$  cubic directions. This is an indication that the films are textured with in-plane rotation. The refractive indices of the thin films were measured using the prism coupling m-line technique and compare favorably with bulk values. Birefringence was observed between TE and TM modes, but was not observed in TE measurements at  $90^\circ$  supporting the conclusion that the films are textured and true in-plane epitaxy has not been achieved. Further work to understand the relationships between growth, microstructure, and loss mechanisms is needed to achieve a thin film material suitable for an efficient SHG device.

## ACKNOWLEDGMENTS

The authors would like to acknowledge; the Office of Naval Research for partial support of this work under contract N00014-91-J-1307, and Bruce Rothman and the Laboratory for Research on the Structure of Matter at the University of Pennsylvania for assistance and use of their equipment in making the RBS measurements under NSF #DMR91-20668.

<sup>1</sup>T. M. Grättinger, S. H. Rou, M. S. Ameen, O. Auciello, and A. I. Kingon, *Appl. Phys. Lett.* **58**, 1964 (1991).

<sup>2</sup>S. Schwyn Thöny and H. W. Lehmann, and P. Günter, *Appl. Phys. Lett.* **61**, 373 (1992).

<sup>3</sup>W. J. Kozlovsky, W. Lenth, E. E. Latta, A. Moser, and G. L. Bona, *Appl. Phys. Lett.* **56**, 2291 (1990).

<sup>4</sup>C. Zimmermann, T. W. Hänsch, R. Byer, S. O'Brien, and D. Welch, *Appl. Phys. Lett.* **61**, 2741 (1992).

<sup>5</sup>C. J. van der Poel, J. D. Bierlein, J. B. Brown, and S. Colak, *Appl. Phys. Lett.* **57**, 2074 (1990).

<sup>6</sup>K. Yamamoto, K. Mizuuchi, and T. Taniuchi, *Optics Lett.* **16**, 1156 (1991).

<sup>7</sup>M. Fujimura, T. Suhara, and H. Nishihara, *Electronics Lett.* **27**, 1207 (1991).

<sup>8</sup>P. Günter, *Appl. Phys. Lett.* **34**, 650 (1979).

<sup>9</sup>M. Amini and M. D. Sacks in *Better Ceramics through Chemistry IV*, (Mater. Res. Soc. Proc. **180**, Pittsburgh, PA, 1990) p. 675.

<sup>10</sup>R. Gutmann and J. Hulliger, *Cryst. Prop. Prep.* **32-34**, 117 (1991).

<sup>11</sup>D. Marcuse, *Theory of Dielectric Optical Waveguides*, (Academic Press, New York, 1974), p. 138.

<sup>12</sup>A. I. Kingon, S. H. Rou, M. S. Ameen, T. M. Grättinger, K. Gifford, and O. Auciello in *Electro-Optics and Non-linear Optic Materials*, edited by A. S. Bhalla, E. M. Vogel, and K. M. Nair (Ceramic Transactions **14**, Westerville, OH, 1990) pp. 179-196.

## **Appendix 4**

## Ferroelectric materials for nonlinear optical devices

---

P. A. MORRIS

DuPont, Central Research & Development  
Wilmington, DE 19880-0356

The properties of interest for applications of crystalline nonlinear optical oxides are often determined by the defect structures introduced in the materials as a result of the processing procedures used to produce the materials. Applications of these types of materials, having high second order nonlinear optical susceptibilities ( $\chi^{(2)}$ ), include frequency convertors, electro-optic modulators and switches, and holographic and phase conjugate optics. Several applications require the fabrication of waveguides or periodic ferroelectric domain structures in the materials. The properties of importance for both bulk crystal and waveguide devices include:  $\chi^{(2)}$ , optical transparency, birefringence and dispersion, ionic and electrical conductivity, optical damage susceptibility, photorefractivity and homogeneity. The defect structures referred to include the intrinsic atomistic defects (e.g. nonstoichiometry), impurities and domains. The growth and processing, defects and resulting properties of several of these materials (e.g.  $\text{KTiOPO}_4$ ,  $\text{KTiOAsO}_4$ ,  $\text{LiNbO}_3$ ,  $\text{KNbO}_3$ ,  $\text{BaTiO}_3$ ,  $\beta\text{-BaB}_2\text{O}_4$ , and  $\text{LiB}_3\text{O}_5$ ) are discussed. Results of studies on these materials indicate that further understanding of the effects of the growth and processing conditions on the resulting defects and properties of bulk nonlinear optical oxide crystals is necessary. Post-growth processing procedures have been used to improve the properties of as-grown materials, but modification of the defects and properties during growth is preferred. Thin films are attractive for many waveguide devices and future integrated optical applications, however the techniques to produce thin films of these materials are currently being developed and little is known about the relationship between the defects present and their properties at this time. The processing-defect-property relationships in nonlinear optical oxides are an important consideration in determining the processing procedures to be used in the development of these materials.